Ocean Sci. Discuss., 12, 1815–1867, 2015
www.ocean-sci-discuss.net/12/1815/2015/
doi:10.5194/osd-12-1815-2015

Ocean Science
Discussions
Open Access

Design and validation of MEDRYS, a Mediterranean Sea reanalysis over 1992–2013

M. Hamon[1], J. Beuvier[1,2], S. Somot[2], J. M. Lellouche[1], E. Greiner[3], G. Jordà[4], M. N. Bouin[2], T. Arsouze[5], K. Béranger[6], F. Sevault[2], C. Dubois[1], M. Drevillon[1], and Y. Drillet[1]

[1]Mercator Océan, 10 rue Hermès, 31520 Ramonville-Saint-Agne, France
[2]Météo France, 42 av. Gaspard Coriolis, 31057 Toulouse CEDEX, France
[3]CLS, 11 rue Hermès, 31520 Ramonville-Saint-Agne, France
[4]Department of Ecology and Marine Resources, IMEDEA (CSIC-UIB), Institut Mediterrani d'Estudis Avançats, Esporles (Illes Balears), Spain
[5]LMD, école Polytechnique, 91128 Palaiseau CEDEX, France
[6]LTHE, rue de la Piscine, 38400 Saint-Martin d'Hère, France

Received: 24 July 2015 – Accepted: 2 August 2015 – Published: 18 August 2015

Correspondence to: J. Beuvier (jonathan.beuvier@mercator-ocean.fr)

Published by Copernicus Publications on behalf of the European Geosciences Union.

Abstract

The French research community on the Mediterranean Sea modelling and the French operational ocean forecasting center Mercator Océan have gathered their skill and expertise in physical oceanography, ocean modelling, atmospheric forcings and data assimilation, to carry out a MEDiterranean sea ReanalYsiS (MEDRYS) at high resolution for the period 1992–2013. The ocean model used is NEMOMED12, a Mediterranean configuration of NEMO with a $1/12^{\circ}$ (~ 7 km) horizontal resolution and 75 vertical z levels with partial steps. At the surface, it is forced by a new atmospheric forcing dataset (ALDERA), coming from a dynamical downscaling of the ERA-Interim atmospheric reanalysis by the regional climate model ALADIN-Climate with a 12 km horizontal and 3 h temporal resolutions. This configuration is used to carry a 34 year free simulation over the period 1979–2013 (NM12-FREE) which is the initial state of the reanalysis in October 1992. The first version of MEDRYS uses the existing Mercator Océan data assimilation system SAM that is based on a reduced-order Kalman filter with a 3-D multivariate modal decomposition of the forecast error. Altimeter data, satellite SST and temperature and salinity vertical profiles are jointly assimilated. This paper describes the configuration we used to perform the MEDRYS simulation. We then first validate the skills of the data assimilation system. It is shown that the data assimilation restores a good averaged temperature and salinity in intermediate layers compared to the free simulation. No particular biases are identified in the bottom layers. However, the reanalysis show slight positive biases of 0.02 psu and 0.15 °C above 150 m depth. In the validation stage, it is also shown that the assimilation allows to better reproduce water, heat and salt transports through the Strait of Gibraltar. Finally, the ability of the reanalysis to represent the sea surface high frequency variability is pointed out.

OSD
12, 1815–1867, 2015

1 Introduction

The Mediterranean Sea is a semi-enclosed sea located between 5.5° W and 36° E and between 30 and 46° N. It is connected to the Atlantic Ocean through the Strait of Gibraltar and to the Black Sea through the Dardanelles and the Bosphorus Straits. The surrounding orography tends to generate cold and dry regional northern winds over the Mediterranean Sea. This leads to strong heat and freshwater losses by evaporation and latent heat transfer. The heat loss is estimated around 5 $\mathrm{W\,m^{-2}}$ (MacDonald et al., 1994) while the freshwater loss is about 0.6 $\mathrm{m\,yr^{-1}}$ (Mariotti et al., 2008). The main part of the heat and water atmospheric losses are balanced by warm Atlantic Waters (AW) entering through the Strait of Gibraltar while it is estimated that only about 10 % of the net water flux is balanced with river runoff (Struglia et al., 2004).

In a climate change context, the Mediterranean area is considered as a hot spot and shows an increase in the temperature and precipitation interannual variability, and a strong warming and drying (Giorgi et al., 2006). The vulnerability of the population is likely to increase with a higher probability of occurrence of events leading to floods and droughts, which are among the most devastating natural hazards. In this context, it is necessary to simulate the water cycle over the Mediterranean basin (Drobinski et al., 2013) and to understand how it will impact water resources. We must improve our understanding of the variability of the water cycle, from extreme events to the seasonal and interannual scales. In addition to the socio-economic motivations and from a strictly physical point of view, the specific configuration of the basin also permits the study of a wide variety of dynamical oceanic processes. For example, the Mediterranean Sea has been found to have a dominant mesoscale circulation component (Robinson et al., 1987; Ayoub et al., 1998; Hamad et al., 2005; Fernandez et al., 2005) in addition to a thermohaline circulation similar to the world ocean (Wüst, 1961; Robinson et al., 2001). The Mediterranean eddy field also shows semi-permanent structures (Rhodes and South Adriatic gyres for example) which define the general circulation in the basin. The time persistency of this small scale field is still an unresolved problem, especially

OSD
12, 1815–1867, 2015

in ocean modelling because for example of approximations and uncertainties on non-linear dynamical balance, atmospheric forcing or the bathymetry (Sorgente et al., 2011; Pinardi et al., 2013).

The ocean reanalysis is a reconstruction technique that allows the production of a consistent four-dimensional estimate of a physical field from observations and numerical modeling simulation. Observations are used to constrain the model trajectory to be near as possible from the “real” state of the ocean. Several techniques have been used in the past to produce large-scale reanalysis but regional reanalysis are challenging because observational datasets are scarcer and the use of high resolution model requires to adequately represent fluxes through the air/sea interface. This is even more important for Mediterranean Sea models in a region surrounded by a various and complex topography. Many small-size islands and a particularly complex coastline limit the low-level air flow, channeling potentially strong and recurring regional winds (Mistral, Tramontane, Bora, Etesian, Sirocco; Herrmann et al., 2011). The role of the spatial resolution of the forcing has been highlighted as a key aspect of the representation of Mediterranean Sea phenomena such as local winds (Sotillo et al., 2005; Ruti et al., 2007; Herrmann et al., 2011; Lebeaupin Brossier et al., 2012), open-sea deep convection (Herrmann and Somot, 2008; Béranger et al., 2010), shelf-cascading (Dufau-Julliand et al., 2004; Langlais et al., 2009), coastal upwelling (Estournel et al., 2009; Casella et al., 2011), permanent circulation features (Estournel et al., 2003; Ourmières et al., 2012) or intermittent eddies (Marullo et al., 2003; Ciappa, 2009; Rubio et al., 2009). The infra-diurnal temporal resolution of the forcing has also been identified as necessary to represent key phenomena such as large salinity anomalies following intense rainfall events (Lebeaupin Brossier et al., 2012) or the SST diurnal cycle (Lebeaupin Brossier et al., 2011, 2014). Other studies demonstrated the importance of the good representation of the atmospheric synoptic chronology linked with the so-called weather patterns or weather regimes (Josey et al., 2011; Papadopoulos et al., 2012; Durrieu de Madron et al., 2013) or with the passage of Mediterranean storms associated with strong air–sea exchanges (Herrmann and Somot, 2008; Herrmann et al., 2010). At a longer time scale, interannual to decadal variability of the atmospheric forcings (water or heat fluxes) is known to dominate the climate variability of the deep water mass formation in both basins of the Mediterranean Sea (Beuvier et al., 2010; Herrmann et al., 2010; L'Heveder et al., 2013) leading sometimes to exceptionnal decadal events such as the Eastern Mediterranean Transient (Roether et al., 2007) or the Western Mediterranean Transition (Schroeder et al., 2008).

The first regional Mediterranean reanalyses, initiated by Oddo et al. (2009), have been recently produced over the 1985–2007 period by Adani et al. (2011), using a reduced-order optimal interpolation and a three-dimensional variational scheme. Their OPA ocean model (Madec et al., 1998) on a $1/16^{\circ}$ regular horizontal grid (Tonani et al., 2008) is forced by daily atmospheric fields from the European Center Medium-Range Weather Forecast (ECMWF) with bulk parameterizations and a monthly precipitation climatology. They used the reanalysis ERA-15 for the 1985–1992 period and then the operational analyses for the 1993–2007 period. We note thus several successive changes in the atmospheric forcing, in particular during the 1993–2007 period, for which the resolution of the ECMWF analyses has progressively increased in several steps from about 100 to 25 km, suggesting then that temporal continuity and coherence in atmospheric forcing were not guaranteed. The first results of these reanalyses pointed out for example that such products allow to better simulate the AW salinity inflow, the sea surface height variability, and current-jet pathways. In the same way of these previous studies, we present in this study another reanalysis of the Mediterranean circulation, MEDRYS, performed with different tools and covering the altimetry 1992–2013 period. Our ocean model used is NEMOMED12 (Beuvier et al., 2012a), a Mediterranean configuration of NEMO (Madec and the NEMO team, 2008; an update version of the OPA code) with the ORCA standard NEMO grid, giving a close horizontal resolution of NEMOMED16. This reanalysis differs also by the use of a reduced-order Kalman filter in the assimilation scheme from the French operational oceanography center Mercator Océan and the long-term 12 km high-resolution fields of the atmospheric forcing called ALDERA. We pay a special attention to the temporal homogene-

OSD
12, 1815–1867, 2015

ity of the atmospheric forcing (same resolution, same model physics) in order to allow robust studies of the interannual to decadal variability of the Mediterranean circulation and trends.

We first present the configuration of the reanalysis in Sect. 2, with the experimental set up, detailing the specifications of the regional configuration of the ocean model, the ALDERA atmospheric forcing and the assimilated dataset. Section 3 presents validation diagnostics and some scientific assessments. Finally, a discussion is conducted on main results and on improvements to be included in further versions of MEDRYS.

2 Experimental set up

2.1 Ocean model configuration: NM12-FREE

We use the ocean general circulation model NEMO (Madec and the NEMO team, 2008) in a regional configuration of the Mediterranean Sea called NEMOMED12 (Lebeaupin Brossier et al., 2011, 2012; Beuvier et al., 2012a, b). The development of NEMOMED12 is made in the continuity of the evolution of the French modeling of the Mediterranean Sea, following OPAMED16 (Beranger et al., 2005), OPAMED8 (Somot et al., 2006) and NEMOMED8 (Beuvier et al., 2010). We describe the NM12-FREE configuration used for the reference 34 year simulation covering the 1979–2013 period and performed with NEMOMED12 without assimilation. More details concerning the physical parametrizations and the boundary conditions of the ocean model are found in Beuvier et al. (2012a).

The NM12 configuration covers the whole Mediterranean Sea and a buffer zone including a part of the Atlantic basin, but not the Black Sea. The horizontal resolution is $1/12^{\circ}$ and corresponds to a varying grid cell size between 6 and 7.5 km (the distance between two points varying with the cosine of the latitude). NM12 has 75 vertical stretched z levels (from $\Delta z = 1$ m at the surface to $\Delta z = 135$ m at the bottom, with 43 levels in the first 1000 m) in a partial step configuration. The bottom layer thickness is varying to fit the bathymetry (Mercator-LEGOS version 10 bathymetry at 1/120° resolution). The no-slip boundary condition is used and the conservation of the model volume is assumed. The mean tidal effect of the quadratic bottom friction formulation computed from a tidal model (Lyard et al., 2006) has been taken into account leading to significant additional bottom friction in the Strait of Gibraltar, Channel of Sicily, Gulf of Gabes and the northern Adriatic sub-basin.

The free simulation NM12-FREE starts in October 1979 and ends in June 2013. Initial conditions are provided by the monthly mean potential temperature and salinity 3-D fields from the state of the MEDATLAS-1979 climatology (Rixen et al., 2005) in the Mediterranean side and from ORAS4 monthly anomalies (Balmaseda et al., 2013) in the Atlantic side. The exchanges with the Atlantic basin are performed through a buffer zone. From 11 to 7.5° W, 3-D temperature and salinity are relaxed toward ORAS4 fields. The restoring term is weak west of Cadiz and Gibraltar areas and increases westwards. As the Mediterranean Sea is an evaporation basin, the model volume is conserved through a damping of the Sea Surface Height (SSH) in the buffer zone toward prescribed SSH anomalies with a very strong restoring. The SSH from ORAS4 is set in the Atlantic according to a strong damping with a very small characteristic time-scale ($\tau = 2$ s).

We use the climatological averages of the interannual dataset of Ludwig et al. (2009) to compute monthly runoff values, split in two parts (Beuvier et al., 2012a). Runoffs from the 33 main rivers are added as precipitation at mouth points whereas the averaged values of the inputs of the other rivers are gathered in each subbasin and put as a coastal runoff. The Black Sea is not included in the NM12-FREE configuration but taken into account with a monthly average one layer net flow across the Marmara Sea and the Dardanelles Strait. We assume that the flow is a freshwater flux (Beuvier et al., 2012a).

OSD
12, 1815–1867, 2015

2.2 Atmospheric forcing: ALDERA

The most recent long-term hindcast simulations using the NEMOMED12 ocean model (Beuvier et al., 2012b; Soto-Navarro et al., 2014; Palmiéri et al., 2015) were driven by the ARPERA2 dataset (Herrmann et al., 2010). This forcing was obtained by a dynamical downscaling using the stretched-grid Regional Climate Model (RCM) ARPEGE-Climate and a spectral nudging technique. ARPERA2 covers the period 1958–2013 with a daily temporal resolution and a 50 km spatial resolution over the Mediterranean Sea. It may include temporal inhomogeneities in the 1970s, a period known for ERA-40 humidity deficiency and in 2001 when the large-scale driving fields changes from ERA-40 to ECMWF analysis.

In order to overcome the main deficiencies of the ARPERA2 dataset (relatively coarse spatial and temporal resolution, temporal homogeneity issue), we have developed a new forcing dataset for the MEDRYS reanalysis. This dataset called ALDERA is based on a dynamical downscaling of the ERA-Interim reanalysis (Dee et al., 2011) over the period 1979–2013 by the RCM ALADIN-Climate (Radu et al., 2008; Colin et al., 2010; Herrmann et al., 2011). We use here the version 5 of ALADIN-Climate firstly described in Colin et al. (2010). For the model definition, we used a Lambert conformal projection for pan-Mediterranean area at the horizontal resolution of 12 km centred at 14° E, 43° N with 432 grid points in longitude and 288 grid points in latitude including the bi-periodization (11) and the relaxation (2 × 8) zones. The model version has 31 vertical levels. The time step used is 600 s. This geographical set-up allows the Med-CORDEX official area (Ruti et al., 2015, www.medcordex.eu) to be fully included in the model central zone. In this configuration, the RCM is driven at its lateral boundary conditions by the ERA-Interim reanalysis (T255, 80 km at its full resolution, Dee et al., 2011, http://www.ecmwf.int/en/research/climate-reanalysis/era-interim) which are updated every 6 h. The ERA-Interim data assimilation system uses a 2006 release of the Integrated Forecasting System, which contains many improvements both in the forecasting model and analysis methodology relative to ERA-40. The period simulated is

OSD
12, 1815–1867, 2015

1979–2013. Before starting this simulation, a two-year long spin-up is carried out allowing the land water content to reach its equilibrium. Land surface parameters and aerosols concentration are updated every month following a climatological seasonal cycle coming from observations. The sea surface temperatures and the sea ice limit (Black Sea) are updated every month with a seasonal and interannual variability following ERA-Interim SST and sea ice analysis. As ERA-Interim constitutes the best knowledge of the 4-D dynamic of the atmosphere available over the last decades, such a simulation is often called "perfect-boundary simulation" or "poor-man regional reanalysis".

ALDERA is available at a 12 km spatial resolution and a 3 h temporal resolution over the whole Mediterranean Sea, Black Sea and near-Atlantic Ocean. It includes a representation of the effect of the aerosols on the long-wave and short-wave radiations and uses the same bulk formula as in ARPERA2 to compute the turbulent fluxes (sensible heat, latent heat and momentum fluxes). To our knowledge, ALDERA is the longest and finest homogeneous atmospheric forcing available for the Mediterranean Sea. All variables required to drive regional ocean models using bulk formula or flux formulation are available. For the MEDRYS reanalysis, the various fluxes have been interpolated every 3 h on the NEMOMED12 grid using a conservative interpolation scheme. All the ALDERA outputs are openly available through the Med-CORDEX database (www.medcordex.eu). Within the frame of the Med-CORDEX initiative, the RCM ALADIN-Climate is also run at lower spatial resolutions (150, 50 km) with exactly the same setting as ALDERA in order to prove the 12 km added-value as illustrated below in Tables 1 and 2 and Figs. 1 and 2.

2.2.1 Long-term Mediterranean Sea surface heat and water budgets

The various terms of the spatially averaged Mediterranean Sea water and heat surface budget are given in Tables 1 and 2 (flux are positive downward in $W\,m^{-2}$ and $mm\,day^{-1}$). References come from Sevault et al. (2014) for the Mediterranean Sea heat budget terms over the 1985–2004 period and from Sanchez-Gomez et al. (2011) for the water budget terms.

Tables 1 and 2 compares the spatially and temporally averaged values of the Mediterranean Sea surface heat and water budget terms of the ALDERA forcing with past studies and observed-based references. ALDERA shows values within the range of the references for the net heat and water surface fluxes, respectively with $-3\,\mathrm{W\,m^{-2}}$ over the 1985–2004 period ($-4\,\mathrm{W\,m^{-2}}$ over the 1979–2012 period) and $-1.69\,\mathrm{mm\,day^{-1}}$ (1979–2011). Both values are in equilibrium with the heat and water transports at the Strait of Gibraltar (see Sect. 3.2.5). However some individual terms show biases. This is especially true for the shortwave radiation, the latent heat flux (and consequently the evaporation) and the precipitation averaged over the sea surface. Note that ALDERA and ARPERA2 show very similar results, what is expected as they share most of their physical parameterizations. This also means that increasing the spatial resolution in the RCMs does not fundamentally change the mean biases at least from 50 to 12 km. This is confirmed when comparing ALDERA to the ALADIN-Climate simulation at 50 km resolution. ALADIN-Climate ran at 150 km is however closer to ERA-Interim with a weaker latent heat loss. Note that Pettenuzzo et al. (2010) dataset also achieves the Mediterranean sea heat budget balance but with lower values both for the shortwave radiation and the latent heat loss. When compared the ENSEMBLES RCMs used in the last published multi-model intercomparison study with Atmosphere RCM (Sanchez-Gomez et al., 2011), ALDERA always fits inside the uncertainty range.

2.2.2 Variability: from the synoptic scale to multi-decadal trends

Sanchez-Gomez et al. (2009) proved that RCMs (including ALADIN-Climate in its version 4) forced by reanalysis over an extended European domain are able to reproduce very well the spatial pattern of the large-scale weather regimes of the driving model as well as their seasonal and interannual variability. However the day-to-day chronology is less well reproduced by the RCMs without spectral nudging. Even if the analysis has not been repeated with the version of ALADIN-Climate used in ALDERA, we are

OSD
12, 1815–1867, 2015
A Mediterranean Sea reanalysis over 1992–2013
M. Hamon et al.

confident that their results are applicable here too as the ALDERA domain is smaller than the ENSEMBLES domain used in their study. Note in addition that the links between the weather pattern and the Mediterranean air–sea fluxes are very strong and now better understood (see Josey et al., 2011; Papadopoulos et al., 2012; Durrieu de Madron et al., 2013).

At the basin scale, the interannual variability of the various terms of the heat fluxes can also be evaluated over the period of the reference dataset (1985–2004, Sevault et al., 2014). For example, for the basin-averaged net shortwave radiation flux, the interannual standard deviation in ALDERA (1.6 $W m^{-2}$) is underestimated with respect to ISCCP observations (2.8 $W m^{-2}$) whereas the interannual temporal correlation is equal to 0.84. For the latent heat loss, the 1985–2004 interannual standard deviation is equal to 5.6 $W m^{-2}$ in ALDERA within the range of the observations (4.7 $W m^{-2}$ for NOCS and 6.7 $W m^{-2}$ for OAFLUX) and the interannual temporal correlation is good (0.83 with NOCS and 0.81 with OAFLUX). Interannual standard deviation are lower for the net longwave radiation flux (1.2 $W m^{-2}$ in ALDERA) and for the sensible heat loss (1.3 $W m^{-2}$ in ALDERA) and the various observation-based estimates disagree (not shown). Concerning the trends in air–sea fluxes, ALDERA does not include yet a trend in the anthropogenic aerosols and therefore does not reproduce the shortwave trend identified in Nabat et al. (2014). However the SST used to drive the RCM does include the observed trend and leads to a realistic positive trend of the latent heat flux though underestimated with respect to Mariotti (2008). Concerning the surface heat flux terms in ALDERA, only the trend in latent heat flux is significant with an increase of the heat loss by the sea equal to +4.1 $W m^{-2} decade^{-1}$ over the 1979–2012 period.

2.2.3 Added-value of the 12 km resolution of ALDERA

Concerning the sea wind representation and the air–sea fluxes, the added-value of the model spatial high resolution has been already demonstrated by various studies (Ruti et al., 2007; Herrmann and Somot, 2008; Béranger et al., 2010; Herrmann et al., 2011; Lebeaupin-Brossier et al., 2012) especially when reaching the 50 km resolution. Her-

OSD
12, 1815–1867, 2015

rmann et al. (2011) show that the 12 km resolution does not bring automatically added-value everywhere, and in particular, in the open ocean, but clearly improves the sea wind representation closer to the coast. Figure 1 illustrates the role of the atmospheric resolution in the representation of the wind and the latent heat flux on 14 March 2013 in the Gulf of Lions by comparing ALDERA at 12 km with ALADIN-Climate runs at lower-resolution. This particular date has been selected because of the strong Mistral event in the Gulf of Lions. Increasing the resolution allows ALDERA to create small-scale features of the wind near the coast as well as the associated pattern of latent heat flux during the Mistral event. The comparison of latent heat flux at 42° N, 5° E also indicates that the maximum of latent heat flux is resolution-dependent. In ALADIN-12 km (the so-called ALDERA), the maximum of latent heat loss is about 900 $W m^{-2}$ whereas in ALADIN-150 km, it barely reaches 500 $W m^{-2}$ with ALADIN-50 km being intermediate.

Figure 2 also illustrates the resolution dependency of the surface wind field but over the Eastern Mediterranean basin during a Meltem (or Etesian) event (16 August 2012). This case shows the clear shadowing effect of the Greek islands. The wind channeling at 12 km leads locally to increased wind speed, changes in wind direction and increased vorticity inputs for the ocean due to strong horizontal gradients. All these effects are visible at the South-Eastern part of Crete, an area where the Ierapetra anticyclone is formed regularly (see below). Note that the goal here is not to prove the added value of the 12 km with respect to lower resolution as in-situ observations and regridded would be required for this purpose but to illustrate differences between the 3 resolutions (150, 50 and 12 km) and to show ALDERA small-scale features with potential impacts on local to regional Mediterranean Sea circulation.

2.3 Data assimilation scheme

The data assimilation system is SAM2 (Système d'Assimilation Mercator 2nd version), which is used at Mercator Océan for operational oceanography purposes. The Mercator Océan monitoring and forecasting system has especially demonstrated its skills within the MyOcean project for the global ocean forecast and we used it in a regional configuration. As the main part of the assimilation scheme used in this paper is already described by Lellouche et al. (2013), we will sum up the assimilation methodology and focus on the specifications inherent to the Mediterranean configuration.

The SAM2 data assimilation method relies on a reduced-order Kalman filter based on the singular evolutive extended Kalman filter (SEEK) with a 7 day assimilation window (hereafter referred as the assimilation cycle). For each assimilation cycle in MEDRYS, SAM2 produces increments of SSH, temperature, salinity and velocity (zonal and meridional components) from the model and the observations, weighted by the forecast error covariance and the specified observation error. Increments are then applied as a tendency term in the model prognostic equations. The forecast error covariance is based on the statistics of a collection of 3-D ocean state anomalies. It relies on a fixed basis seasonally variable ensemble of anomalies. For the Mediterranean configuration, we computed about 900 anomaly fields from the NM12-FREE free simulation for a given assimilation cycle. Compared to a global configuration, the moderate size of the domain allows us to use such a number of anomaly fields (about 300 in a global configuration) in order to statically compute an accurate error covariance field. Moreover, as the analysis increment is a linear combination of the anomalies, a large amount of anomalies is desirable in order to better reproduce the oceanic variability.

In Lellouche et al. (2013), increments of SSH are computed as the sum of barotropic and dynamic height increments (computed from temperature and salinity) in their global configuration. This assumption is only valid far from the coast and in open seas, where the local SSH variations due to the remote wind are negligible. In the Mediterranean Sea, strong regional winds occur in areas with low bathymetry and near important straits like Gibraltar and Sicily. A significant part of SSH is then driven non locally by the wind. Shelf surge and hydraulic control effects are typically 10 times larger in the Mediterranean Sea than in the middle of the ocean. Take into account these wind effects in MEDRYS, we no more use the barotropic plus baroclinic approximation employed in global sytems. As η is a prognostic variable of the model, the SSH increment is computed straight from the η anomaly modes.

OSD
12, 1815–1867, 2015

2.4 Observational datasets

The assimilated observations consist in Sea Surface Temperature (SST) maps, along track Sea Level Anomaly (SLA) data and in situ temperature and salinity profiles. For each cycle, we assimilate the associated centered SST map coming from the daily NOAA Reynolds 0.25° AVHRR-AMSR product (Reynolds et al., 2007). In MEDRYS, we assimilate SST only each 1° to avoid correlation problem between observations. Moreover, we noted a negative average bias of 0.2 °C between AVHRR-AMSR product and the ERA-Interim reanalysis SST that has been used for fluxes computation. For the sake of consistency between fluxes and assimilated SST in MEDRYS, we decided to add 0.2 °C to the AVHRR-AMSR maps as a constant offset.

The along-track SLA is provided by AVISO (SSALTO/DUACS handbook, 2009) and comes from different satellite datasets. Names and acronyms used in this paper as well as the measurement period of each satellite are summarized in Table 3. Small scales signals are removed by filtering the data and a sub-sampling is applied. The filtering and sub-sampling is adapted to each region and product as a function of the characteristics of the area and of the assimilation needs. In the Mediterranean Sea, only one point over two is retained to avoid redundant information (Dufau et al., 2013). The assimilation of SLA observations requires the knowledge of a Mean Dynamic Topography (MDT). The mean surface reference used is a hybrid product between the CNES-CLS09 MDT (Rio et al., 2011) adjusted with GOCE and reanalysis data (Lellouche et al., 2013). In MEDRYS, the effects of the Glacial Isostatic Adjustment (GIA) is taken into account with a correction is about $-0.3\,\mathrm{mm\,yr^{-1}}$. The spatial fluctuations are also applied on the MDT to compensate for the local deformation of the geoid due to the ongoing deformation of the solid Earth (Peltier et al., 2008). For the global ocean in average, the correction is about $-0.3\,\mathrm{mm\,yr^{-1}}$. In addition we also apply a correction to compensate the mass intake of continental ice melting in the Mediterranean basin. On average, the mass intake corresponds to a rise of $0.85\,\mathrm{mm\,yr^{-1}}$.

OSD
12, 1815–1867, 2015

In situ temperature and salinity profiles come from the CORA4 (Cabanes et al., 2013) in situ database provided by CORIOLIS data center from the start of the reanalysis up to December 2012. For the last 6 months we used the real-time database. A check through objective quality control and a data thinning have been done on the dataset in CORA4. Indeed, for each instrument, only one profile per day and within a 0.1° distance is selected. The best profile is identified thanks to a set of objective criteria on measurement resolution and number of validated measurements along the profile. In addition to the quality check done by CORIOLIS, SAM2 carries out a supplementary quality control on in situ observations. In order to minimize the risk of erroneous data being assimilated, the system automatically removes, through different criteria, the data too far from a seasonal climatology (Lellouche et al., 2013).

3 Validation and scientific assessment

The validation of MEDRYS has been done in compliance with a recognized methodology used for global and regional configurations performed within Mercator Océan. As the assimilation system gives us a large amount of information, we first of all check some assimilation statistics. Among the information given, we especially show here statistics on "observation minus forecast" (called innovation) for temperature and salinity profiles, SST and SLA. Then a large number of diagnostics derived from Crosnier and Le Provost (2007) have been produced in order to assess the improvements between MEDRYS and the associated free simulation NM12-FREE. In the following sections, results from the final products (daily outputs for all variables and additional hourly outputs for sea surface variables) are then presented. We first focus on the assimilation of SLA data and its impact on surface circulation. Then, the assessment of the interannual variability is made using integrated heat and salt content. The high frequency surface variability is assessed through a comparison to a fixed mooring in the Gulf of Lions. Finally, we show the effect of the assimilation in terms of transports through the Strait of Gibraltar.

OSD
12, 1815–1867, 2015

3.1 Assimilation statistics

We present here assimilation diagnostics to highlight that the reanalysis system is stable and well constrained by the assimilated observations. In this section, the evolution of the mean and the RMS innovation for all SLA, SST and in situ profiles are shown. The mean and the RMS of SLA innovation are presented in Fig. 3. The mean SLA innovation has a slight linear decrease of 0.65 mm yr^{-1}. This suggests that the volume correction (effect of the GIA and ice melting, see Sect. 2.4) we applied is not accurate enough. On average over the whole period, the mean SLA innovation shows then a slight negative anomaly of −8 mm. We also note a seasonal cycle. This is probably due to inconsistency between ORAS4 interannual SSH fields in the Atlantic part and the assimilated data but a part of this problem could also come from runoff forcing. If the seasonal variations represented in the runoff climatological values are not realistic enough, the error in the intake of water mass through the Mediterranean basin is directly transferred to the SLA innovation. The RMS of the innovation is steady all along the reanalysis and close to 6.5 cm. This result is quite good, knowing that the RMS of observations is 8 cm (not shown here).

The main constraint on the SST consists in the assimilation of in situ surface data and gridded maps derived from satellite measurements. Thus, for each cycle, we assimilate at least 243 values uniformly distributed every spatial degree and a variable amount of in situ data (Fig. 4). Before 2004, we note that the main part of assimilated data comes from the satellite data. The mean satellite SST innovation is close to 0 °C during the whole period of the reanalysis. The RMS of innovation is about 0.7 °C all along the time period and exhibits a seasonal signal with 0.25 °C amplitude whose maximum is reached at the end of summer. The same diagnostic using in situ profile observation at the surface exhibits some similar features but we note a weak positive bias between in situ and satellite data of about 0.12 °C at the end of the period (the RMS and the mean values from in situ measurements are only significant between 2005 and 2012).

OSD
12, 1815–1867, 2015

Finally, we present data assimilation diagnostics for temperature and salinity profiles function of the depth (Figs. 5 and 6). Diagnostics on the amount of assimilated data show that before the Argo era, i.e. before about 2005, there are few profiles deployed in the Mediterranean Sea, and most of them only reach 1000 m depth. This being so, the mean innovation is close to zero in average between the surface and 2000 m depth for temperature and salinity. From 2005 to the end of the experiment, we note a positive anomaly (of observation minus model) of about 0.2 °C and 0.03 psu around 400 m depth. According to Figs. 5 and 6, this seems to result from a propagation of anomalies from surface layers started in 2003. Those positive anomalies at intermediate depths suggest that the Levantine Intermediate Water (LIW) in the model is too cold and too fresh compared to assimilated data in this layer. Conversely, the innovation in surface and deep layers shows a slight negative anomaly. On average, the RMS of the innovation shows reasonable values compared to the mean innovation and the specified observation errors but we note a clear seasonal variation, especially for temperature profiles. During summer, the surface layers become more stratified. Due to the strong gradients, a small variation in the forecast trajectory of the ocean model is then more likely to drift from observations and the RMS naturally increases. Moreover, the cold bias in surface associated to a warm bias in subsurface illustrates that there is a lack of stratification in MEDRYS during summer.

3.2 Scientific assessment results

3.2.1 Mean Sea Surface Height and surface circulation

The Mean Sea Surface Height (MSSH) of the reanalysis and of the associated free simulation NM12-FREE over the period 1993–2012 are compared to the mean surface reference CNES-CLS09 product in Fig. 7. On average over the whole basin, the assimilation has little impact (−2 mm). The impact is strong in term of features. The most important difference concerns the western part of the basin. In NM12-FREE, a significant positive anomaly of MSSH is detected in the Algero-Provençal and the Alboran

OSD
12, 1815–1867, 2015
A Mediterranean Sea reanalysis over 1992–2013
M. Hamon et al.

sub-basin. The strong positive value located North of Majorca Island corresponds to the fingerprint of a too permanent anticyclonic eddy in NM12-FREE (Fig. 8). Thanks to altimetric data, Pascual et al. (2002) identified such an intense eddy in 1998 in the Balearic sub-basin but described it as a temporary event. Actually, in 1998, this anti-cyclonic eddy develops in September due to circumstantial atmospheric and oceanic conditions and disappears during cold seasons. The quasi-permanent occurrence of this eddy in NM12-FREE experiment suggests that the model and its high resolution atmospheric forcing ALDERA are able to produce it but not to dissipate it afterward. This results in a large perturbation in the general circulation in western Mediterranean in NM12-FREE. Indeed, according to Fig. 8, the Liguro-Provençal current in NM12-FREE is deflected at the southern limit of the Gulf of Lions and a significant part of the Atlantic waters is driven along the Spanish coast. This influences the circulation in the Algero-Provençal and the Alboran sub-basins. In MEDRYS, the assimilation process restores realistic SSH and surface circulation. The Atlantic Water (AW) migrates into the western Mediterranean trough the Strait of Gibraltar and reaches the Sicily channel through the Algerian current remaining close to the African coast.

In the reanalysis, the mean kinetic energy especially increases in the Ionian sub-basin compared to the free simulation (Fig. 8). This is partially due to the characteristic of the observation error we used in the assimilation process. The choice has been made not to trust SLA observations within 50 km of the coast and to increase observation errors in these coastal areas. Around the center of the Ionian sub-basin the observation error is not increased and more energy and features are injected by the assimilation process. We also notice that the Levantine sub-basin, and more specifically both the Ierapetra and Pelops anticyclonic eddies, are more energetic suggesting that the mesoscale circulation component have been increased thanks to the assimilation of observational data.

OSD
12, 1815–1867, 2015

3.2.2 Integrated temperature and salinity

Integrated temperature and salinity from the EN3 climatological gridded products (Ingleby and Huddleston, 2007) and the IMEDEA (Mediterranean Institute for Advanced Studies) reconstruction (Jordà et al., 2014) are compared below with MEDRYS and NM12-FREE. Basin integrals of the various products are compared whatever real data is present or not. Monthly evolution over three different layers representing surface (0–150 m), intermediate (150–600 m) and deep (600 m–bottom) waters are shown in Figs. 9 and 10. In this section, observational gridded products will serve as the reference for the heat and salt content. In this validation exercise, we will consider the observational gridded products as the reference.

The time series of the averaged temperature between the surface and 150 m depth point out the good representation of the seasonal cycle in both NM12-FREE and MEDRYS. The phase and the magnitude of the seasonal cycle are consistent with the EN3 and IMEDEA gridded products. In terms of mean value, the two experiments are very close and present a positive bias compared to the gridded products. Indeed, in the 0–150 m layer, the difference between the simulation and EN3 is about 0.15 °C and twice more compared to the IMEDEA reconstruction. This is also consistent with the assimilation statistics of in situ profiles shown in Sect. 3.1. In the upper layer, the averaged salinity in MEDRYS and NM12-FREE is comparable with that in EN3 and the IMEDEA reconstruction. However, between 1992 and 2013, MEDRYS show a slight positive bias of about 0.02 psu whereas NM12-FREE show a slight negative bias of −0.03 psu compared to the reference products. Before 1993, the free simulation presents a clear negative bias of −0.07 psu. In 1993, the data assimilation corrects this surface salinity bias. The interannual variability of the atmospheric water fluxes (Evaporation–Precipitation-Runoffs, not shown) present a less evaporative period followed by a stronger one in the late 90s and early 2000s. This leads to similar variability in the surface salt content in both MEDRYS and NM12-FREE. As there are few in situ data, especially for salinity,

OSD
12, 1815–1867, 2015

the stronger evaporation during the early 2000s leads to high surface salinization in MEDRYS.

Concerning the intermediate waters, one clearly sees the drift of the free simulation. The model in a free configuration tends to warm and salinize intermediate waters. The assimilation of data restores good average values and realistic variability. It is interesting to notice that despite poor data coverage in the early 90s, the assimilation system is able to restore a realistic averaged salinity. As we noted in the previous section, we note a spurious positive anomaly in the MEDRYS salinity in the early 2000s. Those too salty and too dense waters have been formed in the surface layers and have been advected toward the bottom layers. We also detect it in the bottom layers until 2005. Considering the small number of assimilated data below 600 m depth, the model is only slightly constrained beyond this depth, especially before 2005. Thus, the reanalysis is quite close to the free simulation in terms of tendency and mean value for both temperature and salinity.

Concerning the temperature in the deepest layers, it is difficult to establish whether, both the free simulation and the reanalysis, are able to represent a realistic signal. Actually, we cannot clearly distinguish any reference values as the two gridded products show different signals. However, the two experiments present a linear trend of warming of about $4\times10^{-3}\,°\mathrm{C\,yr^{-1}}$ comparable to EN3 for the 1993–2012 period. The IMEDEA reconstruction presents a lower warming of about $1.5\times10^{-3}\,°\mathrm{C\,yr^{-1}}$. In the deepest layer, EN3 and IMEDEA reconstruction show similar mean salinity (respectively 38.63 and 38.64 psu between 1979 and 2010) and a similar interannual variability. NM12-FREE presents a linear salinization over the whole period of the experiment in agreement with the gridded product ($1.2\times10^{-3}\,\mathrm{psu\,yr^{-1}}$). With a limited number of data to assimilate, MEDRYS show an episode of high salinization from 1997 to 2004. Thanks to better data coverage after 2005, the reanalysis becomes more constrained and show a more realistic average salinity, in accordance to our reference products.

OSD
12, 1815–1867, 2015

3.2.3 Temperature and salinity vertical profiles

The model equivalent at the time and spatial location of the observations has been computed from daily averaged outputs. Mean and RMS differences over the whole Mediterranean basin were computed for 3 layers (0–150, 150–600, 600–4000 m) for temperature and salinity profiles (CLASS4 validation; Lellouche et al., 2013). We applied the same process with the profiles from MEDATLAS-1998. The MEDATLAS-1998 temperature and salinity fields are the initial states of short simulations used for process studies such as in Beuvier at al. (2012a). Those fields have been obtained pondering by a low pass filtering with a time-window of three years, the MEDATLAS data covering the 1997–1999 period. The choice of centering the climatology on the late 90s corresponds to a compromise between a recent year (before 2002, the last field in MEDATLAS) and a sufficient data coverage in both temperature and salinity, knowing that the uncertainty associated with the MEDATLAS fields increases after 2000. Only a daily dataset, checked through objective quality control, have been assimilated in MEDRYS. Large differences may appear locally in the CLASS4 scores with spurious observations. CLASS4 results complements here the statistics made against one week forecasts in Sect. 3.1.

We first assess the mean and RMS temperature differences between the analysis and the observation in Fig. 11. Concerning the layer-averaged mean differences, results are not fully consistent with comparisons made with integrated content in Sect. 3.2.2. Indeed, those statistics show that, on average, MEDRYS is very close to the observations (at the location of the observations). We only note a significant negative bias of 0.03 °C in the layer 150/600 m on average over the period 1993–2012. The mean temperature difference in the two first layers of the reanalysis reproduces the interannual variability present in the observations. As MEDATLAS98 is a climatology, the magnitude of the oceanic interannual variability is then represented by the blue curve. We also point out that, in average, no particular temperature bias occurred in the deepest layer in MEDRYS. This highlights that the system is well constrained and efficiently

OSD
12, 1815–1867, 2015

responds to the assimilation of in situ profiles. As in average MEDRYS remains close to temperature measurements, that also confirms that the reference products shown in the Sect. 3.2.2 are subject to uncertainties, especially in the deepest layers where the estimated mean temperature may vary widely from a product to another. In term of mean salinity (Fig. 12), MEDRYS is also close to the observations in the deepest layers but, as expected, presents a slight positive bias of about 0.02 psu between the surface and 150 m depth. When we compared integrated salinity of the reanalysis with other gridded products, we noted a spurious salinization in MEDRYS in the early 2000s that propagated toward deeper layers. In average, the CLASS4 mean difference in salinity is only about 0.1 psu between the surface and 150 m depth and is not noticeable below. This suggests that the signal of the deeper salinization is not in the observations but is a consequence of the propagation of the simulated surface anomaly through the ocean model.

The RMS of the difference is quite good both in temperature and salinity considering the variability in the different layers. However, we note that the RMS of the difference in salinity increases in the waters deeper than 600 m, meaning that, despite a realistic estimation of the mean value, the spatial variability is not robust. This can be explained by the lack of salinity measurements and the poor data coverage in Mediterranean Sea under 1000 m depth, especially before 2005. In average, MEDRYS presents a lower RMS of the difference of temperature and salinity than MEDATLAS98. It is not surprising considering that MEDATLAS98 is composed of climatological monthly fields and does not represent the variability of the Mediterranean Sea along the whole period of 21 years. In the first 150 m, the RMS of the difference in MEDRYS increases with the summertime stratification.

3.2.4 High frequency variability: validation at LION buoy

We assess here the ability of NM12-FREE and MEDRYS to reproduce the high frequency variability at the surface in the Mediterranean basin. In Fig. 13, we compare the high frequency measurements of SST and SSS at the LION buoy (first level of

OSD
12, 1815–1867, 2015

CTD measurements) during HyMeX SOP2 (Special Observation Period 2 from 27 January to 15 March 2013) to the hourly outputs of the two numerical experiments at the same location. As we noted in paragraph 2.4, the real-time database have been assimilated in 2013. Data from LION buoy were not yet available in real-time and were not assimilated. For both SST and SSS comparisons, MEDRYS is slightly closer to the independent observations than the free simulation, in terms of mean values and variability. Indeed, the mean surface water of MEDRYS shows a positive bias of 0.07 °C and 0.03 psu while NM12-FREE shows negative biases which are larger in magnitude (0.13 °C and 0.06 psu). The major part of the mean bias in SSS between MEDRYS and the observations can be explained by the large difference during January (+0.1 psu in average) because the mean bias afterward is very weak (less than 0.01 psu). Indeed, we notice a strong jump in the observed SSS the 30 January (+0.04 psu) corresponding to a salinity sensor repair (M. N. Bouin, personal communication, 2015). The water-pump was defective and affected the conductivity measurement. Assuming that a constant negative bias of 0.04 psu contaminated the observation during January, MEDRYS finally presents very good results in SSS during SOP2 at the LION buoy.

MEDRYS has a better correlation with LION buoy for both SST (75.8 %) and SSS (78.5 %) than NM12-FREE (respectively 31.1 and 78.3 %). For all that, the free simulation is very similar to MEDRYS in the second half of SOP2. This is not surprising since the variability at the surface is controlled by fluxes (identical for both experiments) during the mixed phase of the convection. We especially note the good representation in phase and amplitude of the diurnal variations of SST. This is especially obvious around the 20 February and during many days in March during a temporary restratification period, when the diurnal cycle of ALDERA heat fluxes have a higher daily amplitude (beginning of spring season).

3.2.5 Transport through the Strait of Gibraltar

The Mediterranean Sea is a semi-enclosed basin showing a negative heat and fresh water loss through the air/sea interface. The main part of this loss is balanced by enter-

OSD
12, 1815–1867, 2015

ing heat and water from the Strait of Gibraltar (while only 10 % of the net water flux is due to river runoff). That is why it is necessary to ensure that the fluxes through Gibraltar are realistic. Even if the assimilation scheme corrects a part of the distance between the model and the observation in the Mediterranean Sea, the fluxes play a major role in determining the water mass characteristics and are thereby a good indicator regarding the quality of an experiment over the whole basin. We present here water, heat and salt transport through the Strait of Gibraltar at 5.5° W in Fig. 14. Characteristics of the inflow (surface layers) and the outflow (deep layers) and the difference between the two (net flow) are presented. The interface between inflow and outflow has been determined using the horizontal velocity through the strait at daily time-scale.

Although the characteristics of the ocean are the same in the buffer zone in the two experiments, the amplitude of both inflow and outflow has been improved thanks to data assimilation in MEDRYS (Fig. 14). Despite the realistic value of the net flow through the Strait of Gibraltar, outflow and inflow are underestimated in NM12-FREE in comparison with results published in the last twenty years (Bryden and Kinder, 1991; Bryden et al., 1994; Tsimplis and Bryden, 2000; Candela, 2001; Baschek et al., 2001; Lafuente et al., 2002; Soto-Navarro, 2010). The reason of having a more accurate exchange at Gibraltar in MEDRYS is that the density difference between the inflowing and outflowing waters is larger ($-2.34\,\mathrm{kg\,m^{-3}}$ in MEDRYS and $-2.30\,\mathrm{kg\,m^{-3}}$ in NM12-FREE). In terms of net heat transport, the reanalysis and the free simulation (respectively 6.6 ± 0.4 and $5.5 \pm 0.4\,\mathrm{W\,m^{-2}}$) are consistent with MacDonald et al. (1994). Both averaged temperature and salinity of the inflow in the simulations are also consistent with the characteristics of the ORAS4 Atlantic Water in the buffer zone. We also compare the properties of the inflow in MEDRYS and NM12-FREE with results from Soto-Navarro et al. (2014) at the sill of Espartel. They used, inter alia, the experiment NM12-ARPERA. This simulation show similar results with an interface around 150 m depth. At this particular depth, we also report similar results with AW at 15.4 °C and 36.7 psu in MEDRYS and at 15.5 °C and 36.5 psu in NM12-FREE.

OSD
12, 1815–1867, 2015

The net salt transport through the Strait of Gibraltar at 5.5° W is $1.8 \pm 2.8 \times 10^{-3}$ psu yr^{-1} in MEDRYS and $3.0 \pm 2.6 \times 10^{-3}$ psu yr^{-1} in NM12-FREE (Fig. 14). It directly impacts the salinity of the basin. The trend in salinity of a reference product over the whole basin serves as a way to estimate a reference net salt transport entering at Gibraltar. Using EN3 and the IMEDEA reconstruction, we estimate the net salt intake at approximately 1.7×10^{-3} psu yr^{-1} between 1993 and 2012. In MEDRYS, the averaged net salt transport through the Strait of Gibraltar is very close to this reference value but this is not representative of the evolution of the salinity over the whole basin because of the addition of salinity increments coming from the assimilation scheme. Indeed, NM12-FREE and MEDRYS have a similar trend in salinity in spite of a different net salt transport at Gibraltar.

4 Discussion and conclusion

This study describes the configuration and the quality of the high resolution reanalysis MEDRYS and its companion free simulation NM12-FREE, for the Mediterranean Sea over the period 1992–2013. The common element to both simulations is the ocean model, NEMOMED12, a high-resolution regional configuration of the ocean general circulation model NEMO. The model is relaxed to ORAS4 interannual fields in the Atlantic buffer zone and forced at the surface with the homogeneous and high-resolution ALDERA atmospheric fluxes. The 21 years of the reanalysis have been produced using all available in situ profiles in the CORA4 database, SST maps from the daily NOAA AVHRR-AMSR product and along-track SLA from SSALTO/DUACS associated to SAM2 the assimilation scheme from Mercator Océan. The 12 km and 3 h spatio-temporal resolution of ALDERA fields allows MEDRYS to explicitly reproduce diurnal cycle, and thus SST, and to simulate the impact of local winds on coastal oceanic areas. The consistency of ALDERA dataset along the whole 1979–2013, allows us to trust in the consistency of the interannual variability of processes known to be driven by air–sea interactions (mixed layer variability, surface circulation variability, etc.).

OSD
12, 1815–1867, 2015

The validation process has highlighted the good results of the reanalysis in terms of mean circulation and integrated heat and salt contents. The data assimilation has a positive impact, especially in the western basin, where it restores a correct circulation of the Liguro-Provençal current and of the Algerian current. The assimilation process leads to stronger mesoscale variability in the Ionian and Levantine sub-basin, especially at the location of Ierapetra and Pelops eddies. Looking at in situ profiles, the reanalysis shows a realistic water masses at intermediate depths, unlike in the free simulation. In this layer, the simulation without assimilation NM12-FREE drifts from the observations and show a strong positive trend in both temperature and salinity. Transports through the Strait of Gibraltar have also been improved in the reanalysis. Despite the same forcing in the Atlantic buffer zone, both inflow and outflow in MEDRYS have been increased compared to NM12-FREE and are now comparable to historical values. The net heat and salt budgets through the strait are also consistent with independent products. The improvement of the Atlantic/Mediterranean fluxes at Gibraltar ensures a better budget in the Mediterranean sea.

We showed that surface waters in MEDRYS were in average too salty (about 0.02 psu). This problem probably comes from the adjustment of the volume correction during the computation of SLA model equivalent. Indeed, we noted that the mean SLA innovation (observation minus model forecast) was decreasing of 0.65 mm yr^{-1}, meaning that the simulated sea level tends to rise too quickly compared to the observations. In response thereto, the system tends to compensate by densifying surface waters. As the assimilation system is more constrained on temperature (due to better data coverage) it has a strong effect on salinity. We also point out that it had inconsistencies between ORAS4 interannual fields in the buffer zone and the assimilated data. To correct for those inconsistencies, it will be necessary to apply a correction to the ORAS4 SSH fields in order to better represent the seasonal variations of sea level in the Mediterranean. In further version of MEDRYS, we simply propose to correct the seasonal cycle and the trends of sea level anomalies in ORAS4 in order to match with altimetry observations in the buffer zone.

OSD
12, 1815–1867, 2015

According to additional works (not shown in this study), we realized that SLA innovations were strongly correlated with the mean wind patterns (Mistral-Tramontane, Aegean winds), suggesting that the hydraulic constraint component is not negligible in the Mediterranean Sea. Knowing that, the configuration of SAM2 has been adjusted in order to take into account the wind component in SSH. Moreover, as the effect of the wind at high frequency has been filtered from the SSALTO/DUACS database (SSALTO/DUACS User Handbook, 2014), it will be also necessary to filter it in the model. In order to better assimilate the SLA in Mediterranean Sea, we computed, from MEDRYS outputs, a new empirical observation operator for SLA data. This new configuration takes into account a larger proportion of dynamic height anomaly, determined using a statistical regression over the whole basin. The new model equivalent is then less sensitive to the high frequency wind impact. We conducted some preliminary tests on a particular date, when a strong wind occurred in the Gulf of Lions, and already pointed out the good results in this configuration. All the discussed improvements on the SLA assimilation will be taken into account in a further version of MEDRYS.

In addition to this paper, a comprehensive study process is planned using the further version of MEDRYS. Future work should consider thorough analysis of mechanisms involved in the Mediterranean sea circulation and evolution, using the homogeneous MEDRYS reanalysis. Dense water formation, long term tendencies and water budget have already been identified in the Med-CORDEX/HyMeX frameworks as key issues for Mediterranean dynamical processes and will be part of an oncoming paper.

Acknowledgements. This work is a contribution to the HyMeX program (HYdrological cycle in The Mediterranean EXperiment) through INSU-MISTRALS support and the Med-CORDEX program (COordinated Regional climate Downscaling EXperiment – Mediterranean region). This research has received funding from the French National Research Agency (ANR) project REMEMBER (contract ANR-12-SENV-001).

OSD
12, 1815–1867, 2015

References

Adani, M., Dobricic, S., and Pinardi, N.: Quality assessment of a 1985–2007 Mediterranean Sea reanalysis, J. Atmos. Ocean. Tech., 28, 569–589, doi:10.1175/2010JTECHO798.1, 2011.

Ayoub, N., Le Traon, P.-Y., and De Mey, P.: A description of the Mediterranean surface variable circulation from combined ers-1 and topex/poseidon altimetric data, J. Marine Syst., 18, 3–40, doi:10.1016/S0924-7963(98)80004-3, 1998.

Balmaseda, M. A., Trenberth, K. E., and Källén, E.: Distinctive climate signals in reanalysis of global ocean heat content, Geophys. Res. Lett., 40, 1754–1759, doi:10.1002/grl.50382, 2013.

Baschek, B., Send, U., Garcia Lafuente, J., and Candela, J.: Transport estimates in the Strait of Gibraltar with a tidal inverse model, J. Geophys. Res., 112, 31033–31044, 2001.

Béranger, K., Mortier, L., and Crépon, M.: Seasonal variability of water transport through the Straits of Gibraltar, Sicily and Corsica, derived from a high-resolution model of the Mediterranean circulation, Prog. Oceanogr., 66, 341–364, 2005.

Béranger, K., Drillet, Y., Houssais, M.-N., Testor, P., Bourdallé-Badie, R., Alhammoud, B., Bozec, A., Mortier, L., Bouruet-Aubertot, P., and Crépon, M.: Impact of the spatial distribution of the atmospheric forcing on water mass formation in the Mediterranean Sea, J. Geophys. Res., 115, C12041, doi:10.1029/2009JC005648, 2010.

Beuvier, J., Sevault, F., Herrmann, M., Kontoyiannis, H., Ludwig, W., Rixen, M., Stanev, E., Béranger, K., and Somot, S.: Modeling the Mediterranean Sea interannual variability during 1961–2000: focus on the Eastern Mediterranean Transient, J. Geophys. Res., 115, C08017, doi:10.1029/2009JC005950, 2010.

Beuvier, J., Béranger K., Lebeaupin-Brossier, C., Somot, S., Sevault, F., Drillet, Y., Bourdalle-Badie, R., Ferry, N., and Lyard, F.: Spreading of the Western Mediterranean Deep Water after winter 2005: time scales and deep cyclone transport, J. Geophys. Res.-Oceans, 117, C07022, doi:10.1029/2011JC007679, 2012a.

Beuvier, J., Lebeaupin-Brossier, C., Béranger, K., Arsouze, T., Bourdallé-Badie, R., Deltel, C., Drillet, Y., Drobinski, P., Ferry, N., Lyard, F., Sevault, F., and Somot, S.: MED12, oceanic component for the modeling of the regional Mediterranean Earth System, Mercator Ocean Quaterly Newsletter, 46, 60–66, 2012b.

Bloom, S. C., Takas, L. L., Da Silva, A. M., and Ledvina, D.: Data assimilation using incremental analysis updates, Mon. Weather Rev., 124, 1256–1271, 1996.

Bryden, H. L. and Kinder, T. H.: Steady two-layer exchange through the Strait of Gibraltar, Deep-Sea Res., 38, 445–463, 1991.
Bryden, H. L., Candela, J., and Kinder, T. H.: Exchange through the Strait of Gibraltar, Prog. Oceanogr., 33, 201–248, 1994.
Cabanes, C., Grouazel, A., von Schuckmann, K., Hamon, M., Turpin, V., Coatanoan, C., Paris, F., Guinehut, S., Boone, C., Ferry, N., de Boyer Montégut, C., Carval, T., Reverdin, G., Pouliquen, S., and Le Traon, P.-Y.: The CORA dataset: validation and diagnostics of in-situ ocean temperature and salinity measurements, Ocean Sci., 9, 1–18, doi:10.5194/os-9-1-2013, 2013.
Candela, J.: The Mediterranean water and the global circulation, in: Observing and Modelling the Global Ocean, edited by: Siedler, G., Church, J., and Gould, J., Academic, San Diego, CA, USA, 419–429, 2001.
Casella, E., Molcard, A., and Provenzale, A.: Mesoscale vortices in the Ligurian Sea and their effect on coastal upwelling processes, J. Marine Syst., 88, 12–19, doi:10.1016/j.jmarsys.2011.02.019, 2011.
Ciappa, A. C.: Surface circulation patterns in the Sicily Channel and Ionian Sea as revealed by MODIS chlorophyll images from 2003 to 2007, Cont. Shelf Res., 29, 2099–2109, doi:10.1016/j.csr.2009.08.002, 2009.
Colin, J., Déqué, M., Radu, R., and Somot, S.: Sensitivity study of heavy precipitation in Limited Area Model climate simulations: influence of the size of the domain and the use of the spectral nudging technique, Tellus A, 62, 591–604, doi:10.1111/j.1600-0870.2010.00467.x, 2010.
Crosnier, L. and Le Provost, C.: Inter-comparing five forecast operational systems in the North Atlantic and Mediterranean basins: the MERSEA-strand1 methodology, J. Marine Syst., 65, 354–375, 2007.
Dee, D. P., Uppala, S. M., Simmons, A. J., Berrisford, P., Poli, P., Kobayashi, S., Andrae, U., Balmaseda, M. A., Balsamo, G., Bauer, P., Bechtold, P., Beljaars, A. C. M., van de Berg, L., Bidlot, J., Bormann, N., Delsol, C., Dragani, R., Fuentes, M., Geer, A. J., Haimberger, L., Healy, S. B., Hersbach, H., Hólm, E. V., Isaksen, L., Kållberg, P., Köhler, M., Matricardi, M., McNally, A. P., Monge-Sanz, B. M., Morcrette, J.-J., Park, B.-K., Peubey, C., de Rosnay, P., Tavolato, C., Thépaut, J.-N., and Vitart, F. : The ERA-Interim reanalysis: configuration and performance of the data assimilation system, Q. J. Roy. Meteor. Soc., 137, 553–597, doi:10.1002/qj.828, 2011.

OSD
12, 1815–1867, 2015

A Mediterranean Sea reanalysis over 1992–2013

M. Hamon et al.

Drobinski, P., Ducrocq, V., Alpert, P., Anagnostou, E., Béranger K., Borga, M., Braud, I., Chanzy, A., Davolio, S., Delrieu, G., Estournel, C., Filali Boubrahmi, N., Font, J., Grubisic, V., Gualdi, S., Homar, V., Ivancan-Picek, B., Kottmeier, C., Kotroni, V., Lagouvardos, K., Lionello, P., Llasat, M. C., Ludwig, W., Lutoff, C., Mariotti, A., Richard, E., Romero, R., Rotunno, R., Roussot, O., Ruin, I., Somot, S., Taupier-Letage, I., Tintoré J., Uijlenhoet, R., and Wernli, H.: HyMeX, a 10-year multidisciplinary program on the Mediterranean water cycle, B. Am. Meteorol. Soc., 95, 1063-1082, doi:10.1175/BAMS-D-12-00242.1, 2013.

Dufau-Julliand, C., Marsaleix, P., Petrenko, A., and Dekeyser, I.: Three-dimensional modeling of the Gulf of Lion's hydrodynamics (northwest Mediterranean) during January 1999 (MOOGLI3 Experiment) and late winter 1999: Western Mediterranean Intermediate Water's (WIW's) formation and its cascading over the shelf break, J. Geophys. Res., 109, C11002, doi:10.1029/2003JC002019, 2004.

Durrieu de Madron, X., Hupert, L., Puig, P., Sanchez-Vidal, A., Testor, P., Bosse, A., Estournel, C., Somot, S., Bourrin, F., Bouin, M. N., Beauverger, M., Beguery, L., Calafat, A., Canals, M., Cassou, C., Coppola, L., Dausse, D., D'Ortenzio, F., Font, J., Heussner, S., Kunesch, S., Lefevre, D., Le Goff, H., Martin, J., Mortier, L., Palanques, A., and Raimbault, P.: Interaction of dense shelf water cascading and open-sea convection in the northwestern Mediterranean during winter 2012, Geophys. Res. Lett., 40, 1379–1385, doi:10.1002/grl.50331, 2013.

Estournel, C., Durrieu de Madron, X., Marsaleix, P., Auclair, F., Julliand, C., and Vehil, R.: Observation and modeling of the winter coastal oceanic circulation in the Gulf of Lion under wind conditions influenced by the continental orography (FETCH experiment), J. Geophys. Res., 108, 8059, doi:10.1029/2001JC000825, 2003.

Estournel, C., Auclair, F., Lux, M., Nguyen, C., and Marsaleix, P.: "Scale oriented" embedded modeling of the North-Western Mediterranean in the frame of MFSTEP, Ocean Sci., 5, 73–90, doi:10.5194/os-5-73-2009, 2009.

Fernandez, V., Dietrich, D. E., Haney, R. L., and Tintore, J.: Mesoscale, seasonal and interannual variability in the Mediterranean Sea using a numerical ocean model, Prog. Oceanogr., 44, 321–340, doi:10.1016/j.pocean.2004.07.010, 2005.

Ferry, N., Parent, L., Garric, G., Bricaud, C., Testut, C. E., Le Galloudec, O., Lellouche, J. M., Drevillon, M., Greiner, E., Barnier, B., Molines, J. M., Jourdain, N. C., Guinehut, S., Cabanes, C., and Zawadzki, L.: GLORYS2V1 global ocean reanalysis of the altimetric era (1992–2009) at mesoscale, Mercator Newsletter, 44, 29–39, 2012.

OSD
12, 1815–1867, 2015
A Mediterranean Sea reanalysis over 1992–2013
M. Hamon et al.

Giorgi, F.: Climate change hot-spots, Geophys. Res. Lett., 33, L08707, doi:10.1029/2006GL025734, 2006.
Hamad, N., Millot, C., and Taupier-Letage, I.: A new hypothesis about the surface circulation in the eastern basin of the Mediterranean Sea, Prog. Oceanogr., 66, 287–298, 2005.
Herrmann, M. J. and Somot, S.: Relevance of ERA40 dynamical downscaling for modeling deep convection in the Mediterranean Sea, Geophys. Res. Lett., 35, L04607, doi:10.1029/2007GL032442, 2008.
Herrmann, M., Sevault, F., Beuvier, J., and Somot, S.: What induced the exceptional 2005 convection event in the northwestern Mediterranean basin? Answers from a modeling study, J. Geophys. Res., 115, C12051, doi:10.1029/2010JC006162, 2010.
Herrmann, M., Somot, S., Calmanti, S., Dubois, C., and Sevault, F.: Representation of spatial and temporal variability of daily wind speed and of intense wind events over the Mediterranean Sea using dynamical downscaling: impact of the regional climate model configuration, Nat. Hazards Earth Syst. Sci., 11, 1983–2001, doi:10.5194/nhess-11-1983-2011, 2011.
Ingleby, B. and Huddleston, M.: Quality control of ocean temperature and salinity profiles – historical and real-time data, J. Marine Syst., 65, 158–175, doi:10.1016/j.jmarsys.2005.11.019, 2007.
Josey, S. A., Somot, S., and Tsimplis, M.: Impacts of atmospheric modes of variability on Mediterranean Sea surface heat exchange, J. Geophys. Res., 116, C02032, doi:10.1029/2010JC006685, 2011.
Lafuente, J. G., Delgado, J., Vargas, J. M., Vargas, M., Plaza, F., and Sarhan, T.: Low frequency variability of the exchanged flows through the Strait of Gibraltar during CANIGO, Deep-Sea Res. Pt. II, 49, 4051–4067, 2002.
Langlais, C., Barnier, B., Molines, J. M., Fraunié, P., Jacob, D., and Kotlarski, S.: Evaluation of a dynamically downscaled atmospheric reanalyse in the prospect of forcing long term simulations of the ocean circulation in the Gulf of Lions, Ocean Model., 30, 270–286, doi:10.1016/j.ocemod.2009.07.004, 2009.
Lebeaupin Brossier, C., Béranger, K., Deltel, C., and Drobinski, P.: The Mediterranean response to different space–time resolution atmospheric forcings using perpetual mode sensitivity simulations, Ocean Model., 36, 1–25, doi:10.1016/j.ocemod.2010.10.008, 2011.
Lebeaupin Brossier, C., Béranger, K., and Drobinski, P.: Sensitivity of the northwestern Mediterranean Sea coastal and thermohaline circulations simulated by the 1/12°-resolution ocean

model NEMO-MED12 to the spatial and temporal resolution of atmospheric forcing, Ocean Model., 43–44, 94–107, doi:10.1016/j.ocemod.2011.12.007, 2012.
Lebeaupin Brossier, C., Arsouze, T., Béranger, K., Bouin, M.-N., Bresson, E., Ducrocq, V., Giordani, H., Nureta, M., Rainaud, R., and Taupier-Letage, I.: Ocean mixed layer responses to intense meteorological events during HyMeX-SOP1 from a high-resolution ocean simulation, Ocean Model., 84, 84–103, 2014.
Lellouche, J.-M., Le Galloudec, O., Drévillon, M., Régnier, C., Greiner, E., Garric, G., Ferry, N., Desportes, C., Testut, C.-E., Bricaud, C., Bourdallé-Badie, R., Tranchant, B., Benkiran, M., Drillet, Y., Daudin, A., and De Nicola, C.: Evaluation of global monitoring and forecasting systems at Mercator Océan, Ocean Sci., 9, 57–81, doi:10.5194/os-9-57-2013, 2013.
Le Traon, P. Y., Dibarboure, G., and Ducet, N.: Use of a high resolution model to analyse the mapping capabilities of multiple-altimeter missions, J. Atmos. Ocean. Tech., 18, 1277–1288, 2001.
L'Hévéder, B., Li, L., Sevault, F., and Somot, S.: Interannual variability of deep convection in the Northwestern Mediterranean simulated with a coupled AORCM, Clim. Dynam., 41, 937–960, 2013.
Ludwig, W., Dumont, E., Meybeck, M., and Heussner, S.: River discharges of water and nutrients to the Mediterranean and Black Sea: major drivers for ecosystem changes during past and future decades?, Prog. Oceanogr., 80, 199–217, 2009.
Lyard, F., Lefevre, F., Letellier, T., and Francis, O.: Modelling the global ocean tides: modern insights from FES2004, Ocean Dynam., 56, 394–415, doi:10.1007/s10236-006-0086-x, 2006.
Macdonald, A. M., Candela, J., and Bryden, H. L.: An estimate of the net heat transport through the Strait of Gibraltar, in: Seasonal and Interannual Variability of the Western Mediterranean Sea Coastal and Estuarine Studies, Coastal Estuarine Stud., vol. 46, AGU, Washingtion, DC, USA, 13–32, 1994.
Madec, G. and The-NEMO-Team: NEMO, Technical report (IPSL), France, 2008.
Madec, G., Delecluse, P., Imbard, M., and Levy, C.: OPA, release 8, Ocean general circulation reference manual, Technical Report 96/xx, LODYC/IPSL, France, 1997.
Mariotti, A., Zeng, N., Yoon, J., Artale, V., Navarra, A., Alpert, P., and Li, L.: Mediterranean water cycle changes: transition to drier 21st century conditions in observations and CMIP3 simulations, Environ. Res. Lett., 3, 044001, doi:10.1088/1748-9326/3/4/044001, 2008.

OSD
12, 1815–1867, 2015
A Mediterranean Sea reanalysis over 1992–2013
M. Hamon et al.

Marullo, S., Napolitano, E., Santoleri, R., Manca, B., and Evans, R.: Variability of Rhodes and Ierapetra Gyres during Levantine Intermediate Water Experiment: observations and model results, J. Geophys. Res., 108, 8119, doi:10.1029/2002JC001393, 2003.

Millot, C. and Taupier-Letage, I.: Circulation in the Mediterranean Sea, in: The Handbook of Environmental Chemistry, Vol. 1, Springer-Verlag, 29–66, 2005.

Nabat, P., Somot, S., Mallet, M., Sanchez-Lorenzo, A., and Wild, M.: Contribution of anthropogenic sulfate aerosols to the changing Euro-Mediterranean climate since 1980, Geophys. Res. Lett., 41, 5605–5611, doi:10.1002/2014GL060798, 2014.

Ourmières, Y., Zakardjian, B., Béranger, K., and Langlais, C.: Assessment of a NEMO-based downscaling experiment for the North-Western Mediterranean region: impacts on the Northern Current and comparison with ADCP data and altimetry products, Ocean Model., 39, 386–404, 2011.

Palmiéri, J., Orr, J. C., Dutay, J.-C., Béranger, K., Schneider, A., Beuvier, J., and Somot, S.: Simulated anthropogenic CO_2 storage and acidification of the Mediterranean Sea, Biogeosciences, 12, 781–802, doi:10.5194/bg-12-781-2015, 2015.

Papadopoulos, V. P., Josey, S. A., Bartzokas, A., Somot, S., Ruiz, S., and Drakopoulou, P.: Large-scale atmospheric circulation favoring deep- and intermediate-water formation in the Mediterranean Sea, J. Climate, 25, 6079–6091, doi:10.1175/JCLI-D-11-00657.1, 2012.

Pascual, A., Buongiorno Nardelli, B., Larnicol, G., Emelianov, M., and Gomis, D.: A case of an intense anticyclonic eddy in the Balearic Sea (western Mediterranean), J. Geophys. Res., 107, 3183, doi:10.1029/2001JC000913, 2002.

Peltier, W. R. and Drummond, R.: Rheological stratification of the lithosphere: a direct inference based upon the geodetically observed pattern of the glacial isostatic adjustment of the North American continent, Geophys. Res. Lett., 35, L16314, doi:10.1029/2008GL034586, 2008.

Pettenuzzo, D., Large, W. G., and Pinardi, N.: On the corrections of ERA-40 surface flux products consistent with the Mediterranean heat and water budgets and the connection between basin surface total heat flux and NAO, J. Geophys. Res., 115, C06022, doi:10.1029/2009JC005631, 2010.

Pinardi, N., Zavatarelli, M., Adani, M., Coppini, G., Fratianni, C., Oddo, P., Simoncelli, S., Tonani, M., Lyubartsev, V., Dobricic, S., and Bonaduce, A.: Mediterranean Sea large-scale low-frequency ocean variability and water mass formation rates from 1987 to 2007: a retrospective analysis, Prog. Oceanogr., 132, 318–332, doi:10.1016/j.pocean.2013.11.003, 2013.

Radu, R., Déqué, M., and Somot, S.: Spectral nudging in a spectral regional climate model, Tellus A, 60, 898–910, doi:10.1111/j.1600-0870.2008.00341.x, 2008.
Reynolds, R. W., Smith, T. M., Liu, C., Chelton, D. B., Casey, K. S., and Schlax, M. G.: Daily high-resolution blended analyses for sea surface temperature, J. Climate, 20, 5473–5496, 2007.
Rio, M. H., Guinehut, S., and Larnicol, G.: New CNES-CLS09 global mean dynamic topography computed from the combination of GRACE data, altimetry, and in situ measurements, J. Geophys. Res., 116, C07018, doi:10.1029/2010JC006505, 2011.
Rixen, M., Beckers, J.-M., Levitus, S., Antonov, J., Boyer, T., Maillard, C., Fichaut, M., Balopoulos, E., Iona, S., Dooley, H., Garcia, M.-J., Manca, B., Giorgetti, A., Manzella, G., Mikhailov, N., Pinardi, N., and Zavatarelli, M.: The Western Mediterranean Deep Water: a proxy for climate change, Geophys. Res. Lett., 32, L12608, doi:10.1029/2005GL022702, 2005.
Robinson, A. R., Hecht, A., Pinardi, N., Bishop, J., Leslie, W. G., Rosentroub, Z., Mariano, A. J., and Brenner, S.: Small synoptic/mesoscale eddies and energetic variability of the eastern levantine basin, Nature, 327, 131–134, doi:10.1038/327131a0, 1987.
Robinson, A. R., Leslie, W. G., Theocharis, A., and Laskaratos, A.: Mediterranean Sea circulation, in: Encyclopedia of Ocean Sciences, edited by: Steele, J. H., Thorpe, S. A., and Turekian, K. K., Academic Press, 1689–1706, 2001.
Roether, W., Klein, B., Manca, B. B., Theocharis, A., Kioroglou, S.: Transient Eastern Mediterranean deep waters in response to the massive dense-water output of the Aegean Sea in the 1990s, Prog. Oceanogr., 74, 540–571, doi:10.1016/j.pocean.2007.03.001, 2007.
Rubio, A., Barnier, B., Jordà, G., Espino, M., and Marsaleix, P.: Origin and dynamics of mesoscale eddies in the Catalan Sea (NW Mediterranean): insight from a numerical model study, J. Geophys. Res., 114, C06009, doi:10.1029/2007JC004245, 2009.
Ruti, P., Marullo, S., D'Ortenzio, F., and Tremant, M.: Comparison of analyzed and measured wind speeds in the perspective of oceanic simulations over the Mediterranean basin: analyses, QuikSCAT and buoy data, J. Marine Syst., 70, 33–48, doi:10.1016/j.jmarsys.2007.02.026, 2007.
Ruti, P. M., Somot, S., Giorgi, F., Dubois, C., Flaounas, E., Obermann, A., Dell'Aquila, A., Pisacane, G., Harzallah, A., Lombardi, E., Ahrens, B., Akhtar, N., Alias, A., Arsouze, T., Aznar, R., Bastin, S., Bartholy, J., Béranger, K., Beuvier, J., Bouffies-Cloché, S., Brauch, J., Cabos, W., Calmanti, S., Calvet, J.-C., Carillo, A., Conte, D., Coppola, E., Djurdjevic, V., Drobinski, P., Elizalde-Arellano, A., Gaertner, M., Galàn, P., Gallardo, C., Gualdi, S., Goncalves, M.,

Jorba, O., Jordà, G., L'Heveder, B., Lebeaupin-Brossier, C., Li, L., Liguori, G., Lionello, P., Maciàs, D., Nabat, P., Onol, B., Raikovic, B., Ramage, K., Sevault, F., Sannino, G., Struglia, M. V., Sanna, A., Torma, C., and Vervatis, V.: MED-CORDEX initiative for Mediterranean Climate studies, BAMS, in review, 2015.

Sanchez-Gomez, E., Somot, S., and Déqué, M.: Ability of an ensemble of regional climate models to reproduce weather regimes over Europe-Atlantic during the period 1961–2000, Clim. Dynam., 33, 723–736, 2009.

Sanchez-Gomez, E., Somot, S., Josey, S. A., Dubois, C., Elguindi, N., and Déqué, M.: Evaluation of Mediterranean Sea water and heat budgets simulated by an ensemble of high resolution regional climate models, Clim. Dynam., 37, 2067–2086, 2011.

Schroeder, K., Ribotti, A., Borghini, M., Sorgente, R., Perilli, A., and Gasparini, G. P.: An extensive western Mediterranean deep water renewal between 2004 and 2006, Geophys. Res. Lett., 35, L18605, doi:10.1029/2008GL035146, 2008.

Sevault, F., Somot, S., Alias, A., Dubois, C., Lebeaupin-Brossier, C., Nabat, P., Adloff, F., Déqué, M., and Decharme, B.: A fully coupled Mediterranean regional climate system model: design and evaluation of the ocean component for the 1980–2012 period, Tellus A, 66, 23967, doi:10.3402/tellusa.v66.23967, 2014.

Somot, S., Sevault, F., and Deque, M.: Transient climate change scenario simulation of the Mediterranean Sea for the twenty-first century using a high-resolution ocean circulation model, Clim. Dynam., 27, 851–879, 2006.

Sorgente, R., Olita, A., Oddo, P., Fazioli, L., and Ribotti, A.: Numerical simulation and decomposition of kinetic energy in the Central Mediterranean: insight on mesoscale circulation and energy conversion, Ocean Sci., 7, 503–519, doi:10.5194/os-7-503-2011, 2011.

Sotillo, M. G., Ratsimandresy, A. W., Carretero, J. C., Bentamy, A., Valero, F., and Gonzalez-Rouco, F.: A high-resolution 44-year atmospheric hindcast for the Mediterranean Basin: contribution to the regional improvement of global reanalysis, Clim. Dynam., 25, 219–236, 2005.

Soto-Navarro, J., Criado-Aldeanueva, F., Garcia-Lafuente, J., and Sanchez-Roman, A.: Estimation of the Atlantic inflow through the Strait of Gibraltar from climatological and in situ data, J. Geophys. Res., 115, C10023, doi:10.1029/2010JC006302, 2010.

Soto-Navarro, J., Somot, S., Sevault, F., Beuvier, J., Criado-Aldeanueva, F., Garcia-Lafuente, J., and Béranger, K.: Evaluation of regional ocean circulation models for the Mediterranean Sea at the Strait of Gibraltar: volume transport and thermohaline properties of the outflow, Clim. Dynam., 44, 1277–1292, doi:10.1007/s00382-014-2179-4, 2014.

OSD
12, 1815–1867, 2015

A Mediterranean Sea reanalysis over 1992–2013

M. Hamon et al.

Struglia, M. V., Mariotti, A., and Filograsso, A.: River discharge into the Mediterranean Sea: climatology and aspects of the observed variability, J. Climate, 17, 4740–4751, doi:10.1175/JCLI-3225.1, 2004.
Tsimplis, M. N. and Bryden, H. L.: Estimation of the transport through the Strait of Gibraltar, Deep-Sea Res. Pt. I, 47, 2219–2242, 2000.
Wüst, G.: On the vertical circulation of the Mediterranean Sea, J. Geophys. Res., 66, 3261–3271, doi:10.1029/JZ066i010p03261, 1961.

OSD
12, 1815–1867, 2015
A Mediterranean Sea reanalysis over 1992–2013
M. Hamon et al.

Table 1. Mediterranean Sea averaged and temporal averaged values of the various terms of the sea surface heat budget ($W\,m^{-2}$). Values are computed over the 1985–2004 period except for when indicated. The reference comes from Sevault et al. (2014). The so-called ENSEMBLES RCMs is an ensemble of 15 runs carried out with state-of-the-art RCMs during the EU project ENSEMBLES at 25 km, driven by the ERA-40 reanalysis over the 1958–2001 period (see Sanchez-Gomez et al., 2011).

Dataset	Shortwave	Longwave	Latent heat	Sensible heat	Net surface heat flux
Reference	[183, 185]	[−84, −75]	[−90, −88]	[−14, −6]	[−5, −1]
ALDERA	204	−85	−112	−10	−3
ARPERA2	187	−79	−111	−12	−15
ERA-Int (1989–2004)	198	−83	−97	−12	+6
Pettenuzzo et al. (2010) (1958–2001)	180	−80	−91	−14	−5
ALADIN at 50 km	196	−81	−111	−11	−7
ALADIN at 150 km	200	−82	−94	−10	+14
ENSEMBLES RCMs	[154, 214]	[−100, −70]	[−128, −85]	[−22, −8]	[−40, +21]

OSD
12, 1815–1867, 2015

Table 2. Same as Table 1 but for the Mediterranean Sea surface water budget terms (mm day^{-1}). The reference 1 comes from Sanchez-Gomez et al. (2011) and the reference 2 from Dubois et al. (2010). The reference values do not always cover a common period.

Dataset	Evaporation	Precipitation	River runoff	Black Sea freshwater inputs	Net surface water flux
Reference 1	−3.1	0.7	0.4	0.3	−1.7
Reference 2	[−3.3, −2.9]	[0.6, 0.8]	[0.3, 0.5]	[0.2, 0.4]	[−2.0, −1.4]
ALDERA (1979–2011)	−4.0	1.6	0.4[a]	0.3[a]	−1.7
ARPERA2 (1958–2008)	−3.9	1.8	0.2[b]	0.3[b]	−1.6[b]
ERA-Int (1989–2004)	−3.2	1.4	–	–	
Pettenuzzo et al. (2010) (1958–2001)	−3.2	1.4	–	–	
ALADIN at 50 km (1979–2011)	−4.0	1.4	0.4[a]	0.3[a]	−1.9
ALADIN at 150 km (1979–2011)	−3.3	1.1	0.4[a]	0.3[a]	−1.5
ENSEMBLES RCMs	[−4.4, −2.9]	[1.0, 1.7]	[0.2, 0.6]	[0.1, 0.5]	[−2.0, −1.2]

[a] The ALDERA atmospheric forcing is here completed by the river runoff and Black Sea freshwater inputs coming respectively from Ludwig et al. (2009) and Stanev et al. (2008) as used in Beuvier et al. (2012b) and in the MEDRYS simulation.
[b] The ARPERA2 atmosphere forcing is here completed by the river runoff and Black Sea freshwater inputs coming respectively from Ludwig et al. (2009) and Stanev et al. (2008) as used in the Herrmann et al. (2010) paper.

Table 3. Name, acronym and period of SLA measurement for all satellite used by the assimilation process.

Satellite name	Acronym	Begin	End
ERS2	e2	15 May 1995	09 Apr 2003
Topex/Poseidon	tp	25 Sep 1992	24 Apr 2002
Topex/Poseidon (interleaved)	tpn	16 Sep 2002	08 Oct 2005
Geosat Follow-On	g2	07 Jan 2000	07 Sep 2008
Jason 1	j1	24 Apr 2002	19 Oct 2008
Envisat	en	09 Oct 2002	22 Oct 2010
Jason 2	j2	19 Oct 2008	now
Jason 1 (interleaved)	j1n	14 Feb 2009	now
Envisat (interleaved)	enn	22 Oct 2010	now
Cryosat 2	c2	19 Feb 2012	now
Jason 1 Geodetic	j1g	14 May 2012	now

OSD
12, 1815–1867, 2015

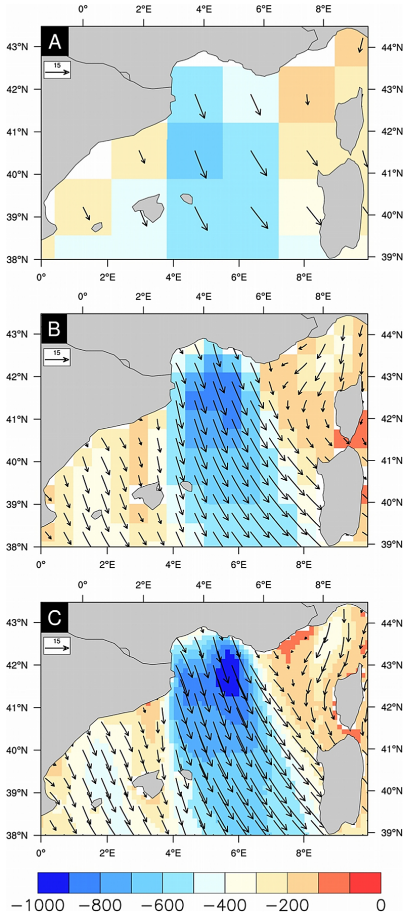

Figure 1. Daily average wind direction (arrows) and latent heat flux (color in $\mathrm{W\,m^{-2}}$) on 14 March 2013 in **(a)** ALADIN-150 km, **(b)** ALADIN-50 km and **(c)** Aladin-12 km (the so-called ALDERA).

OSD

12, 1815–1867, 2015

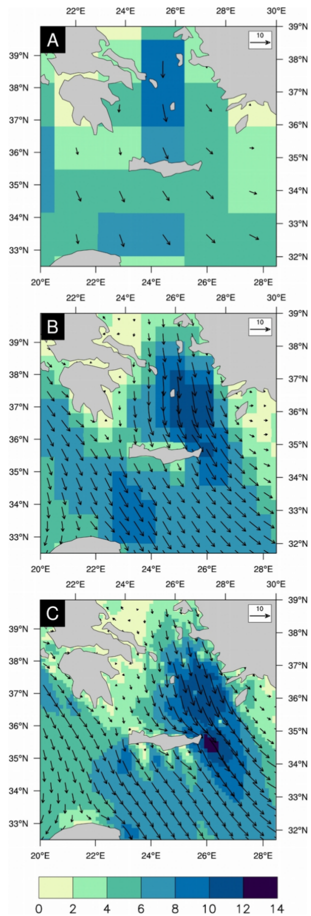

Figure 2. Daily average wind direction (arrows) and wind speed (color in $m\,s^{-1}$) on 16 August 2012 in **(a)** ALADIN-150 km, **(b)** ALADIN-50 km and **(c)** ALADIN-12 km (the so-called ALDERA).

OSD
12, 1815–1867, 2015

A Mediterranean Sea reanalysis over 1992–2013

M. Hamon et al.

Title Page
Abstract | Introduction
Conclusions | References
Tables | Figures
◂◂ | ▸▸
◂ | ▸
Back | Close
Full Screen / Esc
Printer-friendly Version
Interactive Discussion

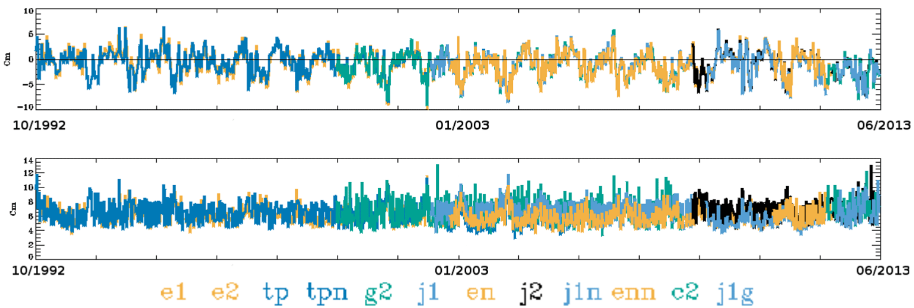

Figure 3. Time series of weekly sea level anomaly (SLA, m) data assimilation statistics averaged over the whole Mediterranean basin: mean innovation (top) and RMS of innovation (bottom). The colors stand for different satellites (please refer to Table 3).

OSD
12, 1815–1867, 2015

A Mediterranean Sea reanalysis over 1992–2013

M. Hamon et al.

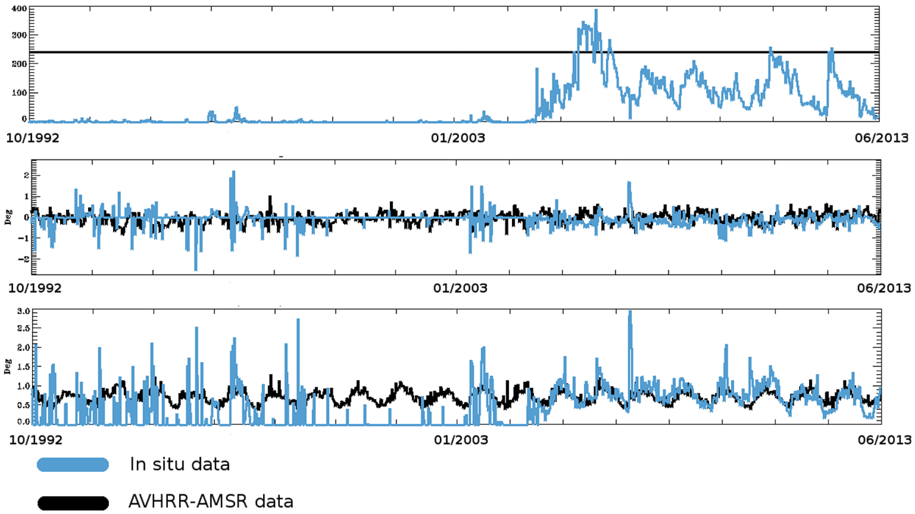

Figure 4. Time series of weekly sea surface temperature (SST, °C) data assimilation statistics from in situ (blue) and satellite SST AVHRR-AMSR (black), averaged over the whole Mediterranean basin: number of data (top), mean innovation (middle) and RMS of innovation (bottom).

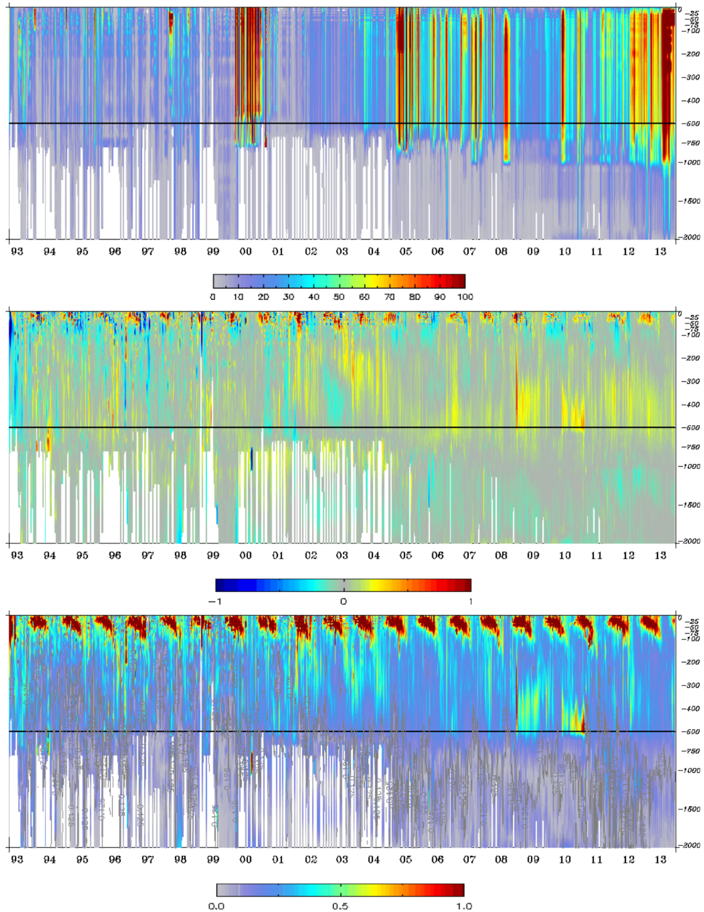

Figure 5. Evolution of weekly temperature data assimilation statistics from in situ profiles, function of the depth averaged over the whole Mediterranean basin: number of profiles (top), mean innovation (middle) and RMS of the innovation (bottom).

OSD

12, 1815–1867, 2015

A Mediterranean Sea reanalysis over 1992–2013

M. Hamon et al.

Title Page
Abstract | Introduction
Conclusions | References
Tables | Figures
◀I | ▶I
◀ | ▶
Back | Close
Full Screen / Esc
Printer-friendly Version
Interactive Discussion

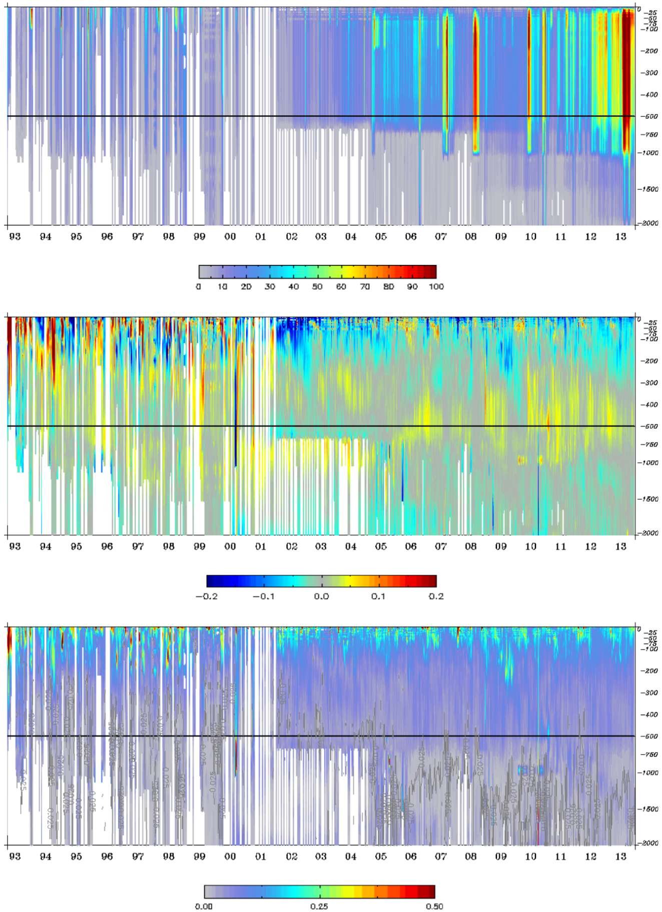

Figure 6. Evolution of weekly salinity data assimilation statistics from in situ profiles, function of the depth averaged over the whole Mediterranean basin: number of profiles (top), mean innovation (middle) and RMS of the innovation (bottom).

OSD
12, 1815–1867, 2015

A Mediterranean Sea reanalysis over 1992–2013

M. Hamon et al.

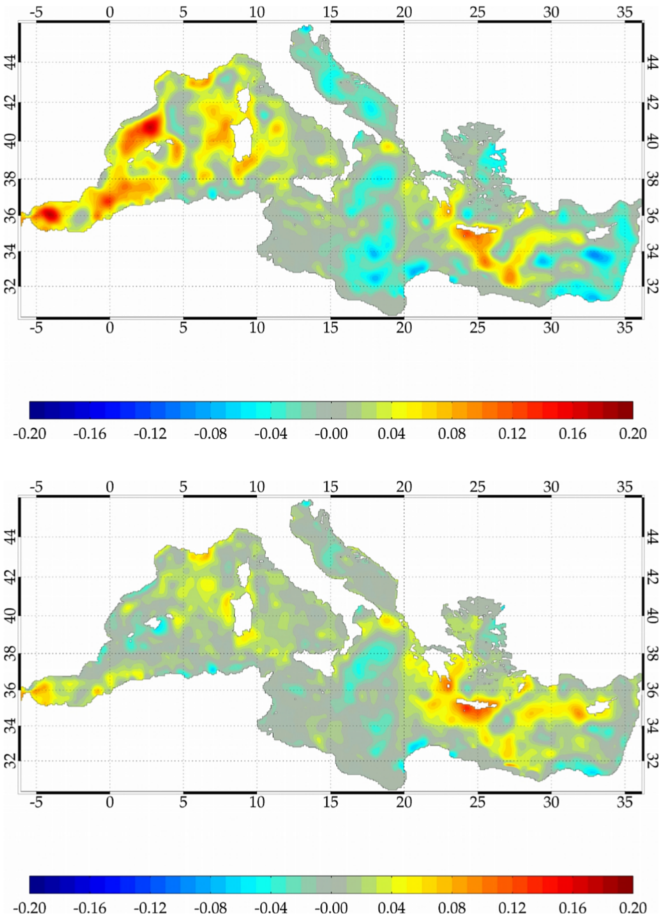

Figure 7. Difference (in cm) between the Mean Sea Surface Height of NM12-FREE over the period 1993–2012 (top) and MEDRYS1V1 (bottom) and the mean surface reference CNES-CLS09.

OSD
12, 1815–1867, 2015

A Mediterranean Sea reanalysis over 1992–2013

M. Hamon et al.

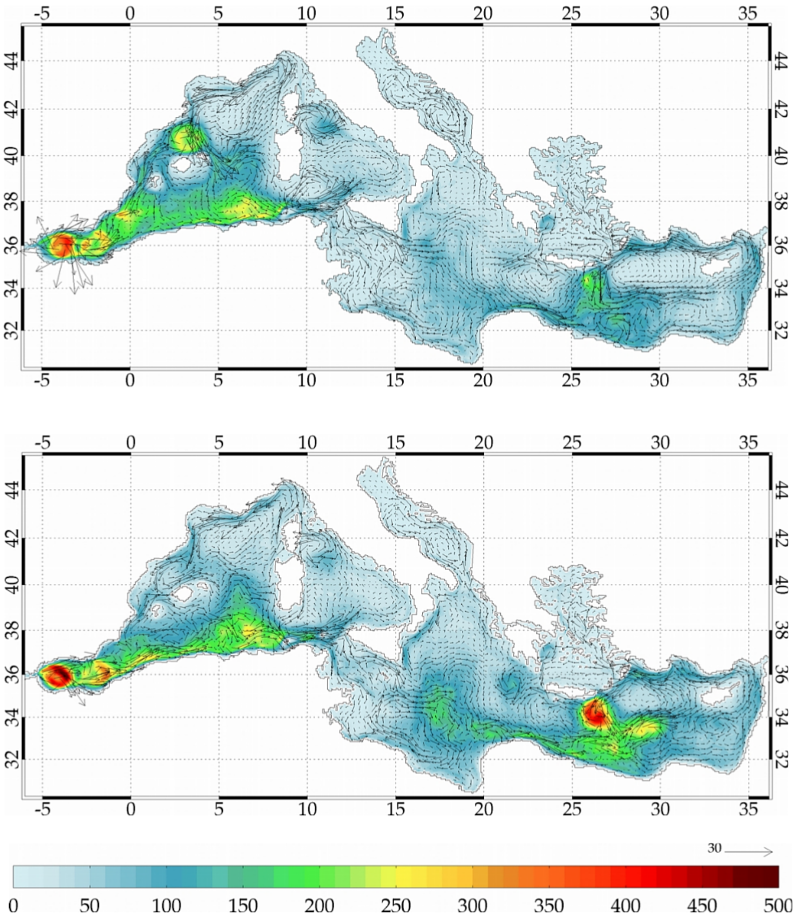

Figure 8. Mean Eddy Kinetic Energy (EKE in $cm^2 s^{-2}$) at 40 m depth over the period 1992–2013 for NM12-FREE (top) and MEDRYS1V1 (bottom). Arrows represent the mean currents (in $cm^2 s^{-1}$) over the same period and at the same depth.

OSD
12, 1815–1867, 2015

Title Page
Abstract | Introduction
Conclusions | References
Tables | Figures
◀| |▶
◀ ▶
Back | Close
Full Screen / Esc
Printer-friendly Version
Interactive Discussion

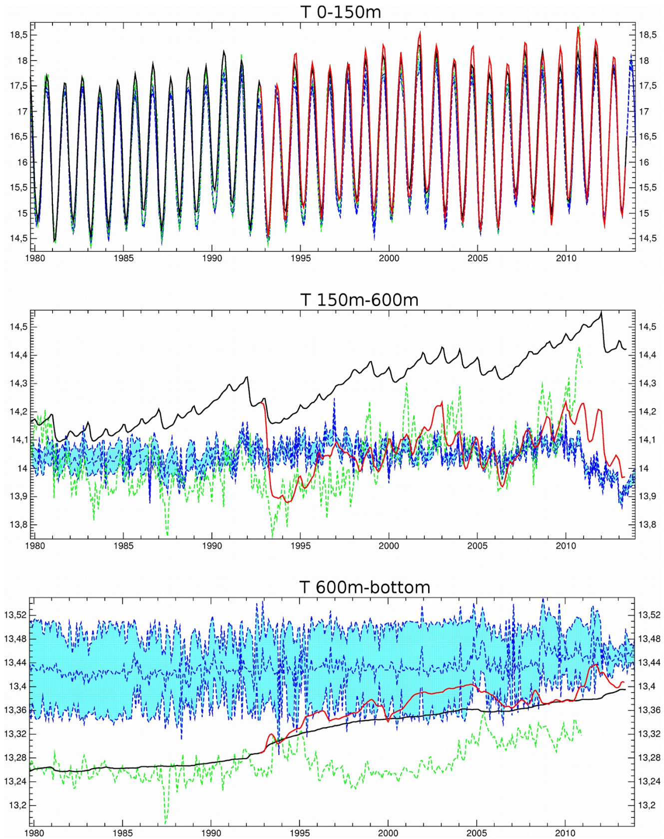

Figure 9. Evolution of the monthly integrated heat content (expressed as mean temperature in °C) over the Mediterranean basin for the layers 0–150 m (top), 150–600 m (middle) and 600 m–bottom (bottom) from MEDRYS1V1 (red line), NM12-FREE (black line), EN3 (dotted green line) and the IMEDEA (blue dotted line) hydrographic gridded products. The blue shaded area indicates the uncertainty ranges around the values of the IMEDEA reconstruction.

OSD
12, 1815–1867, 2015

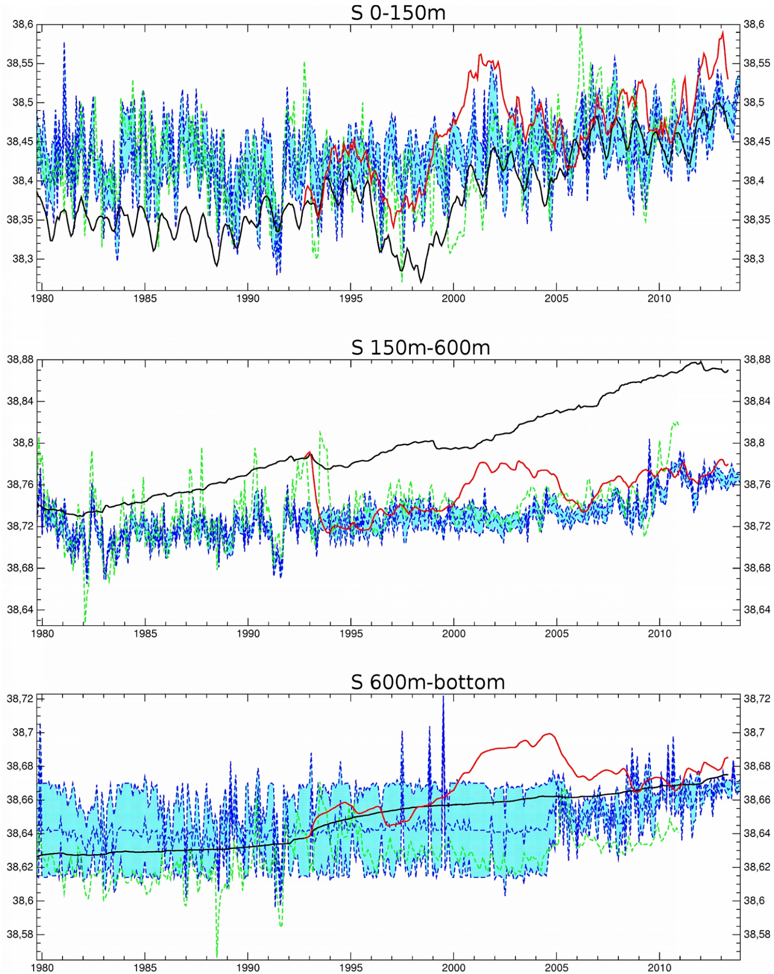

Figure 10. Same as Fig. 9 but for integrated salt content (expressed as mean salinity in psu).

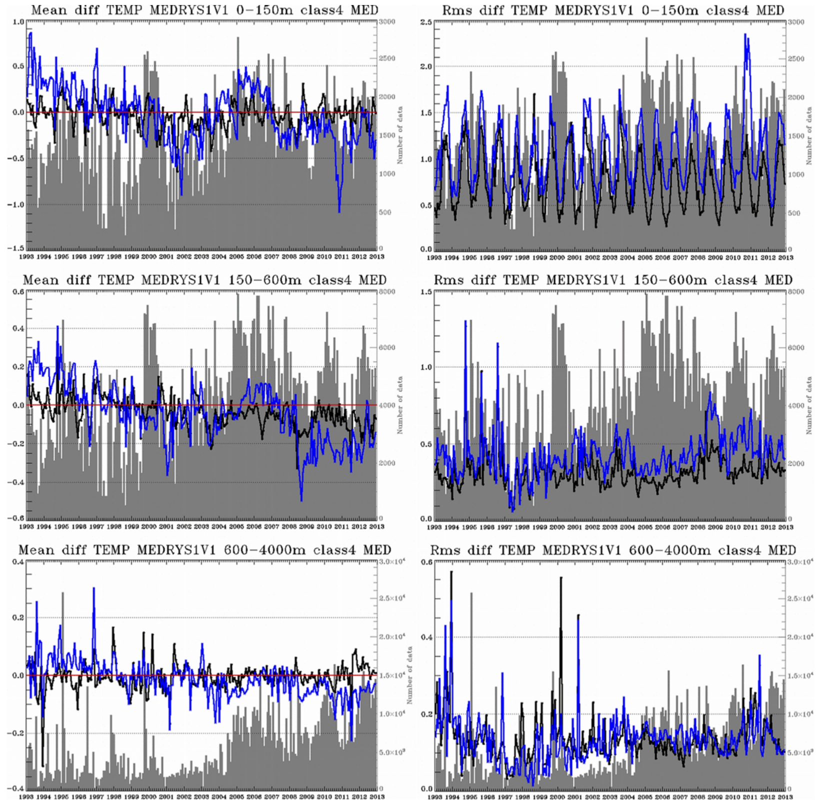

Figure 11. Temperature (°C) mean (upper row) and RMS (bottom row) differences between analysis and observation (black), and between MEDATLAS98 and observation (blue). For these diagnostics, all available T/S observations from the CORIOLIS database and MEDRYS1V1 daily average analysis, collocated (temporally and spatially) with observations, are used. The number of observations is shown with gray bars. Averages are performed in the 0–150 m (left), 150–600 m (middle) and 600–4000 m (right) layers in the whole Mediterranean basin.

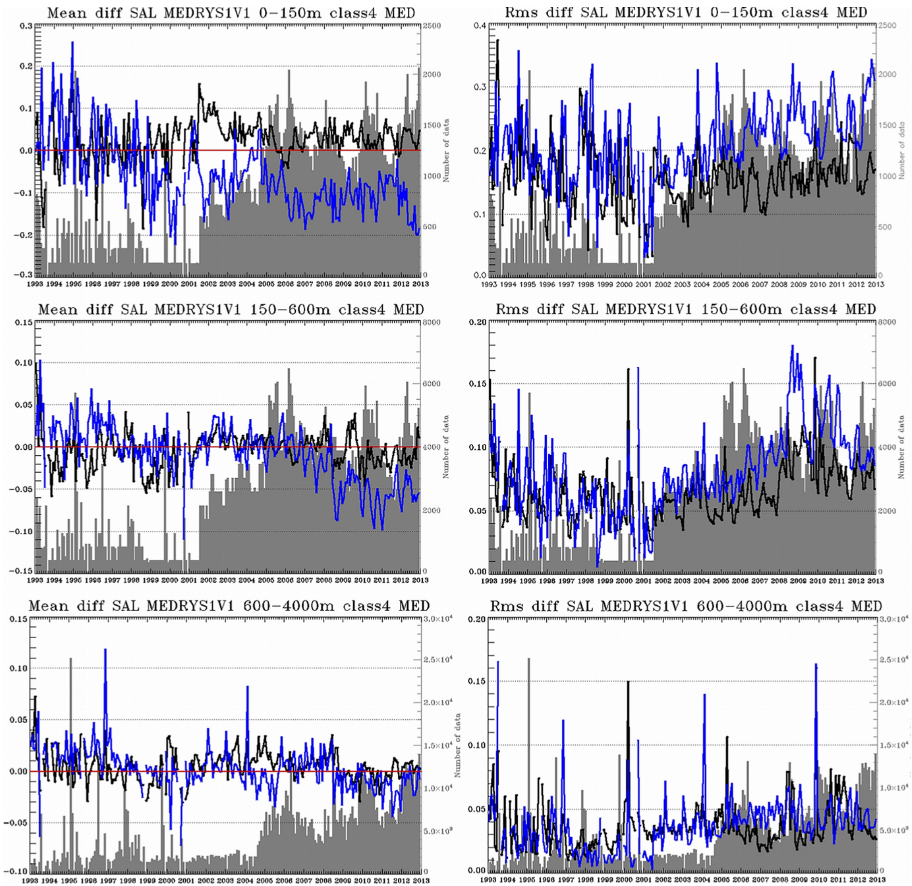

Figure 12. Same as Fig. 11 but for salinity (psu).

OSD
12, 1815–1867, 2015

A Mediterranean Sea reanalysis over 1992–2013

M. Hamon et al.

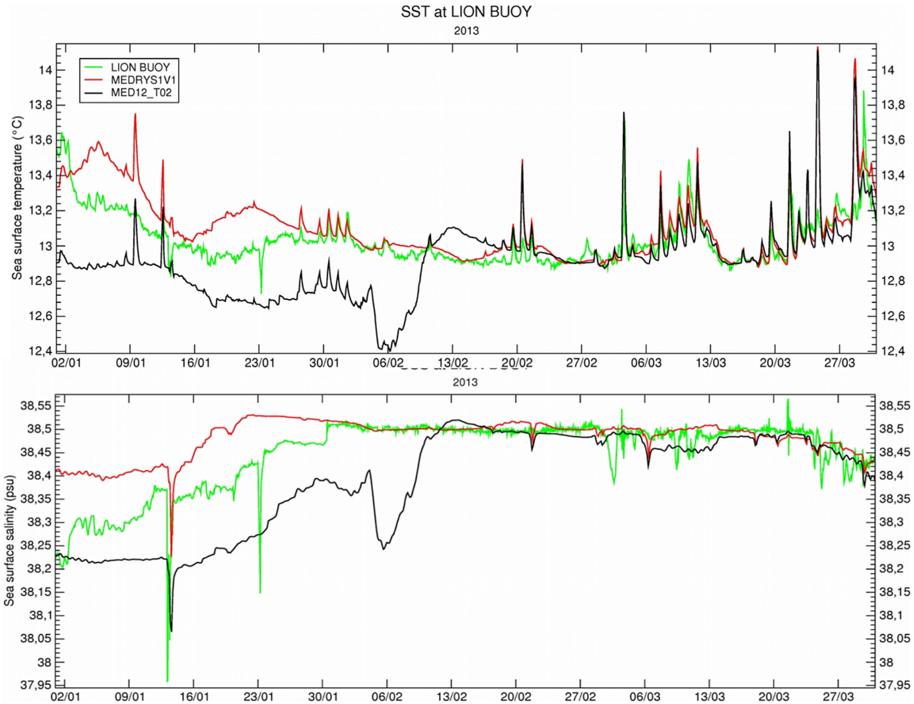

Figure 13. Evolution of the hourly Sea Surface Temperature (SST, top) and Sea Surface Salinity (SSS, bottom) at the LION buoy location between 1 January and 31 March 2013. The observation is shown with the green lines, NM12-FREE with the black lines and MEDRYS1V1 with the red lines.

OSD

12, 1815–1867, 2015

A Mediterranean Sea reanalysis over 1992–2013

M. Hamon et al.

	IN	OUT	NET
Water *(Sv)*			
NMED12-FREE	+0.70 ± 0.03	-0.65 ± 0.03	+0.047 ± 0.009
MEDRYS1V1	+0.81 ± 0.03	-0.77 ± 0.03	+0.048 ± 0.009
Heat *(W/m²)*			
NMED12-FREE (averaged temperature)	+19.6 ± 0.9 17.18 °C	-14.1 ± 0.6 13.62 °C	+5.5 ± 0.4 (diff = +3.56 °C)
MEDRYS1V1 (averaged temperature)	+22.8 ± 0.9 17.13 °C	-16.2 ± 0.6 13.31 °C	+6.6 ± 0.4 (diff = +3.82 °C)
Salt *(10^{-3} psu/year)*			
NMED12-FREE (averaged salinity)	+208 ± 8 36.49 psu	-205 ± 9 38.44 psu	+3.0 ± 2.6 (diff = -1.95 psu)
MEDRYS1V1 (averaged salinity)	+243 ± 9 36.54 psu	-241 ± 10 38.45 psu	+1.8 ± 2.8 (diff = -1.91 psu)

Figure 14. Average flow, heat and salt transport of the inflow and the outflow through the Strait of Gibraltar at 5.5° W between 1992 and 2013 for NMED12-FREE and MEDRYS1V1. The uncertainty corresponds to the annual standard deviation. For heat and salt transport, the associated mean temperature and salinity in the layer are specified. The green color represents values consistent with literature or/and reference products and the red color, those that are not consistent.

OSD
12, 1815–1867, 2015